NUREG/CR-4029
ANL-84-68

NUREG/CR-4029
ANL-84-68

LOCAL FORMULATION OF INTERFACIAL AREA CONCENTRATION AND ITS MEASUREMENTS IN TWO-PHASE FLOW

by

Isao Kataoka, Mamoru Ishii,
and Akimi Serizawa

ARGONNE NATIONAL LABORATORY, ARGONNE, ILLINOIS
Operated by THE UNIVERSITY OF CHICAGO

Prepared for the Office of Nuclear Regulatory Research
U. S. NUCLEAR REGULATORY COMMISSION
under Interagency Agreement DOE 40-550-75

Argonne National Laboratory, with facilities in the states of Illinois and Idaho, is owned by the United States government, and operated by The University of Chicago under the provisions of a contract with the Department of Energy.

NUREG/CR-4029
ANL-84-68
(Distribution Codes: R2 & R4)

ARGONNE NATIONAL LABORATORY
9700 South Cass Avenue
Argonne, Illinois 60439

LOCAL FORMULATION OF INTERFACIAL AREA CONCENTRATION AND ITS MEASUREMENTS IN TWO-PHASE FLOW

by

Isao Kataoka,* Mamoru Ishii,
and Akimi Serizawa**

Reactor Analysis and Safety Division

Report Completed: July 1984

Report Issued: October 1984

Prepared for the Division of Accident Evaluation
Office of Nuclear Regulatory Research
U. S. Nuclear Regulatory Commission
Washington, D. C. 20555
under Interagency Agreement DOE 40-550-75

NRC FIN No. A2026

* Institute of Atomic Energy, Kyoto University, Uji, Kyoto 611, Japan.
**Dept. of Nuclear Engineering, Kyoto University, Sakyo-ku, Kyoto 606, Japan.

LOCAL FORMULATION OF INTERFACIAL AREA CONCENTRATION AND ITS MEASUREMENTS IN TWO-PHASE FLOW

by

Isao Kataoka,* Mamoru Ishii, and Akimi Serizawa**

ABSTRACT

The interfacial area concentration is one of the most important parameters in analyzing two-phase flow based on the two-fluid model. The local instantaneous formulation of the interfacial area concentration is introduced here. Based on this formulation, time and spatial averaged interfacial area concentrations are derived, and the local ergodic theorem (the equivalency of the time and spatial averaged values) is obtained for stationary developed two-phase flow. On the other hand, the global ergodic theorem is derived for general two-phase flow. Measurement methods are discussed in detail in relation to the present analysis. The three-probe method, with which local interfacial area concentration can be measured accurately, has been proposed. The one probe method under some statistical assumptions has also been proposed.

In collaboration with the experimental data for the interfacial velocity, radial profiles of the local interfacial area concentration are obtained based on the one probe method. The result indicates that the local interfacial area concentration has a peak value near the tube wall in bubbly flow, while in slug flow it shows a higher value in the central region of the tube for that particular set of data.

NRC
FIN No.
A2026

Title
Phenomenological Modeling of Two-phase Flow in Water Reactor Safety Research

*Institute of Atomic Energy, Kyoto University, Uji, Kyoto 611, Japan.

**Department of Nuclear Engineering, Kyoto University, Sakyo-ku, Kyoto 606, Japan.

TABLE OF CONTENTS

	Page
ABSTRACT	ii
NOMENCLATURE	vi
EXECUTIVE SUMMARY	1
I. INTRODUCTION	2
II. LOCAL INSTANTANEOUS INTERFACIAL AREA CONCENTRATION	7
A. Spatial Averaging of Interfacial Area	10
B. Time Averaging of Interfacial Area	15
C. Ergodic Hypothesis of Interfacial Area Concentration	18
III. MEASUREMENT METHODS OF LOCAL INTERFACIAL AREA CONCENTRATION	21
IV. EXPERIMENTAL VALUE OF LOCAL INTERFACIAL AREA CONCENTRATION	37
V. CONCLUSIONS	47
ACKNOWLEDGMENTS	51
REFERENCES	52
APPENDIX A	56

LIST OF FIGURES

No.	Title	Page
1	Local Interfacial Area Concentration in One Dimension	8
2	Angle Between $\vec{n}_z$ (z Direction) and $\vec{n}_j$	12
3	Angle Between $\vec{v}_{ij}$ and $\vec{n}_j$	12
4	Double Sensored Probe and jth Interface	22
5	Three Double Sensored Probes	25
6	Angles α_j and β_j for $\vec{v}_{ij}$	29
7	Angles μ_j and ν_j for $\vec{n}_j$	30
8	Spectra of $\|v_{sz}\|$ for Air-Water Bubbly Flow at j_g = 0.135 m/s and j_ℓ = 1.03 m/s at Various Radial Positions (Serizawa et al. [55,57])	38
9	Radial Profiles of N_t, $1/\overline{(1/\|v_{sz}\|)}$ and $\sigma_{sz}/\overline{\|v_{sz}\|}$ for Air-Water Bubbly Flow at j_g = 0.135 m/s and j_ℓ = 1.03 m/s (Serizawa et al. [55,57])	40
10	Radial Profile of $\bar{a}_i^t$ for Air-Water Bubbly Flow at j_g = 0.135 m/s and j_ℓ = 0.442 m/s Calculated from the Data of Serizawa et al. [55,57]	41
11	Radial Profile of $\bar{a}_i^t$ for Air-Water Bubbly Flow at j_g = 0.135 m/s and j_ℓ = 0.737 m/s Calculated from the Data of Serizawa et al. [55,57]	42
12	Radial Profile of $\bar{a}_i^t$ for Air-Water Bubbly Flow at j_g = 0.135 m/s and j_ℓ = 1.03 m/s Calculated from the Data of Serizawa et al. [55,57]	43
13	Radial Profile of $\bar{a}_i^t$ for Air-Water Bubbly Flow at j_g = 0.268 m/s and j_ℓ = 1.03 m/s Calculated from the Data of Serizawa et al. [55,57]	44
14	Radial Profile of $\bar{a}_i^t$ for Air-Water Bubble-to-Slug-Transition Flow at j_g = 0.268 m/s and j_ℓ = 0.737 m/s Calculated from the Data of Serizawa et al. [55,57]	45

LIST OF FIGURES (Cont'd)

No.	Title	Page
15	Radial Profile of $\bar{a}_i^t$ for Air-Water Slug Flow at j_g = 0.402 m/s and j_ℓ = 1.03 m/s Calculated from the Data of Serizawa et al. [55,57]	46
16	Radial Profiles of $\bar{a}_i^t$, $\bar{\alpha}$ (Void Fraction) and $\tilde{u}_\ell$ (Turbulent Velocity of Liquid) at j_g = 0.135 m/s and j_ℓ = 1.03 m/s (Serizawa et al. [55,57])	48

NOMENCLATURE

NOMENCLATURE

a_i	Interfacial area concentration
$a_i(x)$	Local interfacial area concentration (one dimensional)
$a_i(x,y,z,t)$	Local instantaneous interfacial area concentration
$\bar{a}_i^p$	Spatial averaging of $a_i(x,y,z,t)$
$\bar{a}_i^{p1}$	Linear averaging of $a_i(x,y,z,t)$
$\bar{a}_i^{p2}$	Surface averaging of $a_i(x,y,z,t)$
$\bar{a}_i^{p3}$	Volume averaging of $a_i(x,y,z,t)$
$\bar{a}_i^{pz}$	Linear (z direction) averaging of $a_i(x,y,z,t)$
$\bar{a}_i^t$	Time averaging of $a_i(x,y,z,t)$
$A(x,y)$	Function of x and y
$A_0 \sim A_3$	Determinant given by Eqs. (78) and (80) to (82)
$B(x,y)$	Function of x and y
$\overline{(1/\cos\theta)}$	Reciprocal of harmonic mean of $\cos\theta_j$ (Eq. (33))
$\cos\theta_x$, $\cos\theta_y$, $\cos\theta_z$	Direction cosines of ds or normal vector of dS
$\cos\eta_x$, $\cos\eta_y$, $\cos\eta_z$	Direction cosines of $\vec{n}_s$
$\cos\eta_{xk}$, $\cos\eta_{yk}$, $\cos\eta_{zk}$	Direction cosines of $\vec{n}_{sk}$
$f(x,y,z,t)$	Function representing a interface
$f_j(x,y,z,t)$	Function representing jth interface
$\vec{g}$	Acceleration due to gravity
$g(\alpha)$	Probability density function of α
$\vec{g}rad\ f$, $\vec{g}rad\ f_j$	Gradient of $f(x,y,z,t)$ and $f_j(x,y,z,t)$
h_{ki}	Heat transfer coefficient at interface
$h(\beta)$	Probability density function of β
H_k	Enthalpy of k phase
$I(V,\Omega)$	Integration of $a_i(x,y,z,t)$ in domain V and Ω
$I(L,\Omega)$	Integration of $a_i(x,y,z,t)$ in domain L and Ω
j_g, j_ℓ	Superficial velocity for gas and liquid
ℓ	Length scale given by Eq. (30), reciprocal of number of interfaces per unit length
L	Length in z direction
L_s	Length scale at interface given by Eq. (4)
$\dot{m}_k$	Mean mass transfer per unit area for k phase
M_{ik}	Interfacial force for k phase
n	Number
$\vec{n}_j$	Unit normal vector of jth interface
$\vec{n}_s$	Unit vector in the direction of probe
$\vec{n}_{sk}$	Unit vector in the direction of kth probe
$\vec{n}_x$, $\vec{n}_y$, $\vec{n}_z$	Unit vector of x, y, and z direction
N_t	Number of bubbles or droplets passing a point per unit time
N_z	Number of bubbles or droplets per unit length
P_k	Pressure of k phase
$P(\theta)$	Probability density function of θ
$P(\alpha,\beta,\mu,\nu)$	Probability density function of α, β, μ, ν
$P(\alpha,\mu,(\beta-\nu))$	Probability density function of α, μ, $(\beta-\nu)$
$\bar{q}_k$	Mean conduction heat flux of k phase
q_k^t	Turbulent heat flux of k phase
$q_{ki}^{\cdot}$	Interfacial heat flux
r	Radial position
R	Radius of flow passage
s	Linear coordinate

S	Surface
t	Time when average is taken
t_0	Fixed time
t_j	Time given by Eq. (41)
T	Time
T_i	Temperature at interface
T_k	Bulk temperature of k phase
$\tilde{u}_\ell$	Turbulence velocity of liquid phase
$\vec{v}_{ij}$	Velocity of jth interface
$\overline{\lvert\vec{v}_i\rvert}$, $\overline{\lvert\vec{v}_i\rvert^2}$	Arithmetric mean of $\lvert\vec{v}_{ij}\rvert$ and $\lvert\vec{v}_{ij}\rvert^2$
$\overline{\frac{1}{\lvert\vec{v}_i\rvert}}$	Reciprocal of harmonic mean of $\lvert\vec{v}_{ij}\rvert$
$\overline{\frac{1}{\lvert\vec{v}_i\rvert\cos\phi}}$	Reciprocal of harmonic mean of $\lvert\vec{v}_{ij}\rvert\cos\phi_j$
$\vec{v}_{ixj}$, $\vec{v}_{iyj}$, $\vec{v}_{izj}$	x,y, and z component of $\vec{v}_{ij}$
$\bar{\vec{v}}_{ix}$, $\bar{\vec{v}}_{iy}$, $\bar{\vec{v}}_{iz}$	Arithmetric mean of $\vec{v}_{ixj}$, $\vec{v}_{iyj}$, and $\vec{v}_{izj}$
$\overline{\lvert\vec{v}_{ix}\rvert^2}$, $\overline{\lvert\vec{v}_{iy}\rvert^2}$, $\overline{\lvert\vec{v}_{iz}\rvert^2}$	Arithmetric mean of $\lvert\vec{v}_{ixj}\rvert^2$, $\lvert\vec{v}_{iyj}\rvert^2$, and $\lvert\vec{v}_{izj}\rvert^2$
$\vec{v}_k$	Velocity of k phase
v_s, v_{sj}	Passing velocity of jth interface through double sensored probe
v_{skj}	Passing velocity of jth interface through kth double sensored probe
v_{szj}	Passing velocity of jth interface through double sensored probe in z direction
$\overline{\frac{1}{\lvert v_{sz}\rvert}}$	Reciprocal of harmonic mean of $\lvert v_{szj}\rvert$ (Eq. (118))
$\overline{\lvert v_{sz}\rvert}$	Arithmetric mean of $\lvert v_{szj}\rvert$
V	Volume
$w(\lvert v_{sz}\rvert)$	Probability density function of $\lvert v_{sz}\rvert$
x, y, z	Coordinates
x_0, y_0, z_0	Fixed point in x, y, and z coordinate
z_j	z coordinate given by Eq. (25)
z	Axial coordinate

Greek Symbols

$\bar{\alpha}$	Void fraction
α_k	Volume fraction of k phase
α_j	Angle between $\vec{v}_{ij}$ and $\vec{n}_z$
α_0	Angle given by Eq. (102)
β_j	Angle between $\vec{n}_y$ and projection of $\vec{v}_{ij}$ into x-y plane
γ	Constant
Γ_k	Mass generation of k phase
$\delta(x)$	Delta function
Δt, Δt_j, Δt_{jk}	Time lag of (jth) interface passing between sensor 1 and 2 of (kth) double sensored probe
Δx	Spacing in x direction
Δs	Distance between sensor 1 and 2 of double sensored probe
θ_j	Angle between $\vec{n}_z$ and $\vec{n}_j$
μ_j	Angle between $\vec{n}_z$ and $\vec{n}_j$
ν_j	Angle between $\vec{n}_y$ and projection of $\vec{v}_{ij}$ into x-y plane
ξ_j	Angle between $\vec{n}_s$ and $\vec{n}_j$
ρ_k	Density of k phase
σ_x, σ_y, σ_z, σ_{sz}	Root mean square of fluctuating components of $\vec{v}_{ixj}$, $\vec{v}_{iyj}$, $\vec{v}_{izj}$ and $\lvert v_{szj}\rvert$

τ	Time scale given by Eq. (46), reciprocal of number of interfaces passing a point per unit time
τ_i	Average interfacial shear stress
$\bar{\bar{\tau}}_k$	Average viscous stress for k phase
τ_k^t	Turbulent shear stress for k phase
d_j	Angle between $\vec{n}_j$ and $\vec{v}_{ij}$
$\phi(x)$	Arbitrary function
ϕ_k	Energy dissipation for k phase
Ω	Time duration

Subscripts

f	Liquid phase
g	Gas phase
i	Value at interface
k	k phase (gas or liquid)

EXECUTIVE SUMMARY

Recently two-phase flow analyses based on a two-fluid model formulation have been applied to some engineering problems, particulary in the area of safety evaluations of light water reactor and fast breeder reactor. This is because the two-fluid model is considered to be the most accurate model among the models available today. In theory it can predict two-phase flow phenomena under transient and developing conditions better than previous mixture models such as the homogeneous or drift flux model.

In the two-fluid model formulation, interfacial transfer terms which couple equations for gas and liquid are quite important. In terms of the first order effects, these interfacial transfer terms are proportional to the interfacial area concentration (area of gas-liquid interface in unit volume). Therefore, an accurate correlation for the interfacial area is indispensable for two-phase flow analyses based on the two-fluid model.

However, the knowledge of the interfacial area concentration is quite limited due to considerable difficulties in experimental measurements. Particularly, there is little knowledge on the local interfacial area concentration in spite of its necessity in two or three dimensional analyses. In view of this, the local interfacial area concentration has been studied in detail both theoretically and experimentally in this report.

The local instantaneous formulation of the interfacial area concentration has been obtained. It can be applied to any two-phase flow regime. Based on the formulation, spatial and time averaged interfacial area concentrations have been derived in terms of observable parameters of two-phase flow. For stationary and developed two-phase flow, it has been proved that the time averaging and spatial averaging are equivalent in terms of both local and overall values. This fact is quite important in practical application because one can measure the local interfacial area concentration by time averaging of observed signals obtained by a local probe.

New measurement methods for the interfacial area concentration are indicated based on the presently developed theory. A three-probe method which gives a measurement of the local interfacial area concentration is proposed and discussed in detail. A one-probe method based on some statistical assumptions of two-phase flow characteristics is also proposed and discussed. This method is proven to be practical and quite useful. Using this

measurement technique, one can measure the local interfacial area concentration with considerable accuracy when some statistical characteristics of interfacial motions are known.

The above one-probe method is applied to experimental data of interfacial velocities. From this, transverse profiles of local interfacial area concentration are obtained for bubbly and slug flow. In bubbly flow, the local interfacial area concentration indicated a ringwise peak near the wall for these experiments. On the other hand, in slug flow the local interfacial area concentration had a peak value at the center.

The proposed measurement methods can be applied to obtain a broad data base for modeling the interfacial area concentration. They can be used for both local and area averaged interfacial area concentrations. Such experiments will be quite useful for developing accurate constitutive relations for interfacial transfer terms. The present research has established a firm theoretical base for these measurements as well as demonstrated the applicability of the methods by obtaining the experimentally measured interfacial area concentrations in two-phase flow.

I. INTRODUCTION

In order to analyze the thermal-hydraulics of two-phase flow, various formulations such as the homogeneous flow model, drift-flux model [1-3], and two-fluid model have been proposed [4,5]. Among these models, the two-fluid formulation can be considered the most accurate model because of its detailed treatment of the phase interactions at the interface. The two-fluid model is formulated by considering each phase separately in terms of two sets of conservation equations which govern the balance of mass, momentum, and energy of each phase. These balance equations represent the macroscopic fields of each phase and are obtained from proper averaging methods. Since the macroscopic fields of each phase are not independent of the other phase, the phase interaction terms which couple the transport of mass, momentum, and energy of each phase appear in the field equations. It is expected that the two-fluid model can predict mechanical and thermal nonequilibrium between phases accurately. In particular, for transient or entrance flow involving acceleration of one phase with respect to the other, inertia terms of each phase should be considered separately by use of the two-fluid model. However, it is noted that

the interfacial transfer terms should be modeled accurately for the two-fluid model to be useful. In the present state of the arts, the constitutive equations for these interfacial terms are the weakest link in the two-fluid model. The difficulties arise due to the complicated transfer mechanisms at the interfaces coupled with the motion and geometry of the interfaces. Furthermore, the constitutive equations should be expressed by macroscopic variables based on proper averaging.

As has been shown in detail [4], the interfacial transfer terms in a two-fluid model appear as averaging of local instant transfers of mass, momentum, and energy. However, these terms appear as source terms in the field equations, therefore, it is necessary to model each term by identifying proper transport mechanisms and using experimental data.

A three-dimensional two-fluid model has been obtained by using temporal or statistical averaging [4]. The model is expressed in terms of two sets of conservation equations governing the balance of mass, momentum, and energy in each phase. For most practical applications, the model developed by Ishii [4] can be simplified to the following forms:

Continuity Equation

$$\frac{\partial \alpha_k \rho_k}{\partial t} + \nabla \cdot (\alpha_k \rho_k \vec{v}_k) = \Gamma_k \tag{1}$$

Momentum Equation

$$\frac{\partial \alpha_k \rho_k \vec{v}_k}{\partial t} + \nabla \cdot (\alpha_k \rho_k \vec{v}_k \vec{v}_k) = -\alpha_k \nabla p_k + \nabla \cdot \alpha_k (\bar{\bar{\tau}}_k + \tau_k^t)$$

$$+ \alpha_k \rho_k \vec{g} + \vec{v}_{ki} \Gamma_k + \vec{M}_{ik} - \nabla \alpha_k \cdot \tau_i \tag{2}$$

Enthalpy Energy Equation

$$\frac{\partial \alpha_k \rho_k H_k}{\partial t} + \nabla \cdot (\alpha_k \rho_k H_k \vec{v}_k) = -\nabla \cdot \alpha_k (\bar{\bar{q}}_k + q_k^t) + \alpha_k \frac{D_k}{Dt} p_k$$

$$+ H_{ki}\Gamma_k + \frac{q''_{ki}}{L_s} + \Phi_k \tag{3}$$

Here Γ_k, $\vec{M}_{ik}$, τ_i, q''_{ki}, and Φ_k are the mass generation, generalized interfacial drag, interfacial shear stress, interfacial heat flux, and dissipation, respectively. The subscript k denotes k phase, and i stands for the value at the interface. L_s denotes the length scale at the interface, and $1/L_s$ has the physical meaning of the interfacial area per unit volume [4]. Thus,

$$\frac{1}{L_s} = a_i = \frac{\text{Interfacial Area}}{\text{Mixture Volume}} \tag{4}$$

The above field equations indicate that several interfacial transfer terms appear on the right-hand sides of the equations. Since these interfacial transfer terms also should obey the balance laws at the interface, interfacial transfer conditions could be obtained from an average of the local jump conditions [4]. They are given by

$$\sum_k \Gamma_k = 0$$

$$\sum_k \vec{M}_{ik} = 0 \tag{5}$$

$$\sum_k \left(\Gamma_k H_{ki} + q''_{ki}/L_s\right) = 0$$

Therefore, constitutive equations for $\vec{M}_{ik}$, q''_{gi}/L_s, and q''_{fi}/L_s are necessary for the interfacial transfer terms. The enthalpy interfacial transfer condition indicates that specifying the heat flux at the interface for both phases is equivalent to the constitutive relation for Γ_k if the mechanical-energy transfer terms can be neglected [4]. This aspect greatly simplifies the development of the constitutive relations for interfacial transfer terms.

By introducing the mean mass transfer per unit area, m_k, defined by

$$\Gamma_k \equiv a_i m_k \,, \tag{6}$$

the interfacial energy-transfer term in Eq. (3) can be rewritten as

$$\Gamma_k H_{ki} + \frac{q''_{ki}}{L_s} = a_i \left(m_k H_{ki} + q''_{ki} \right) \tag{7}$$

The heat flux at the interface should be modeled using the driving force or the potential for an energy transfer. Thus,

$$q''_{ki} = h_{ki} \left(T_i - T_k \right) \tag{8}$$

where T_i and T_k are the interfacial and bulk temperatures based on the mean enthalpy. A similar treatment of the interfacial momentum transfer term is also possible. In view of the above, the importance of the interfacial area, a_i, in developing constitutive relation for this term is evident. The interfacial transfer terms are now expressed as a product of the interfacial area and the driving force. It is essential to make a conceptual distinction between the effects of these two parameters. The interfacial transfer of mass, momentum, and energy increases with an interfacial-area concentration toward the mechanical and thermal equilibrium.

Thus, in general, the interfacial transfer terms are given in terms of the interfacial area concentration a_i and driving force [4,6,7] as

$$\text{(Interfacial Transfer Term)} = a_i \times \text{(Driving Force)} \tag{9}$$

The area concentration defined as the interfacial area per unit volume of the mixture characterizes the geometrical effects; therefore, it must be related to the structure of the two-phase flow field. On the other hand, the driving forces for the interfacial transport characterize the local transport mechanisms such as the turbulent and molecular diffusions.

In two-phase flow systems, the void fraction and interfacial area concentration are two of the most important geometrical parameters. The void

fraction is treated as a variable to be solved from a set of balance equations, whereas the interfacial area concentration should be specified by a constitutive relation or by introducing an additional transport equation for a_i [4,6]. As the above formulation indicates, the knowledge of the interfacial area concentration is indispensable in the two-fluid model.

Although a number of studies [6-43] have been made in this area, the interfacial area concentration in two-phase flow has not been sufficiently investigated both experimentally and analytically. Most of the previous studies are for steady state flow without phase change. Available experimental data are limited to volume averaged interfacial area concentration over a section of a flow channel. Detailed review of these are given in Refs. [6] and [7]. There are a number of shortcomings in measurement techniques. Furthermore, there are very few established theoretical foundations for relating this interfacial area to some easily measurable quantities. In particular, there seems to be no information available on a local value of the interfacial area concentration. However, this local interfacial area concentration is very important for two or three dimensional analyses using the two-fluid model.

There is one problem dealing with the definition of the interfacial area concentration locally and instantaneously. Since the Lebesgue measure of an interface is zero, the local instantaneous interfacial area concentration cannot be represented by an ordinary function [44,45]. To avoid this problem, an integral method has been used in the analysis of the interfacial area [4,5]. However, by introducing a distribution which is a generalized function [44, 45], one can express the local instantaneous interfacial area concentration.

Based on this local instantaneous formulation and the assumptions of the statistical characteristics of two-phase flow, fundamental relations for the interfacial area concentration have been derived. These equations relate the local value of the interfacial area to observable parameters of the two-phase flow. Based on this theory, some measurement techniques of the local interfacial area concentration have been proposed. Finally, using the existing experimental data on flow measurements, radial profiles of the local interfacial concentration have been obtained.

II. LOCAL INSTANTANEOUS INTERFACIAL AREA CONCENTRATION

By considering a simple system shown in Fig. 1, where there is only one gas-liquid interface, the location of the interface is represented by

$$x = x_o \tag{10}$$

Now a control volume is defined by

$$\gamma - \frac{\Delta x}{2} \leq x \leq \gamma + \frac{\Delta x}{2} \tag{11}$$

Then the spatial averaged interfacial area concentration $\bar{a}_i^p$ in the control volume, is given by

$$\begin{aligned} \bar{a}_i^p &= \frac{1}{\Delta x} \quad \text{for} \quad |\gamma - x_o| < \frac{\Delta x}{2} \\ &= 0 \quad \text{for} \quad |\gamma - x_o| > \frac{\Delta x}{2} \end{aligned} \tag{12}$$

By taking the limit of $\Delta x \to 0$, the local interfacial area concentration $a_i(x)$ in a one-dimensional form is given by

$$a_i(x) = \delta(x - x_o) \tag{13}$$

Here $\delta(x - x_o)$ is the delta function [44-46] which satisfies

$$\int_{-\infty}^{\infty} \delta(x - x_o)dx = 1 \quad , \quad \delta(x - x_o) = 0 \text{ for } x \neq x_o \tag{14}$$

One of the special characteristics of the delta function is that for any smooth function $\phi(x)$, it gives

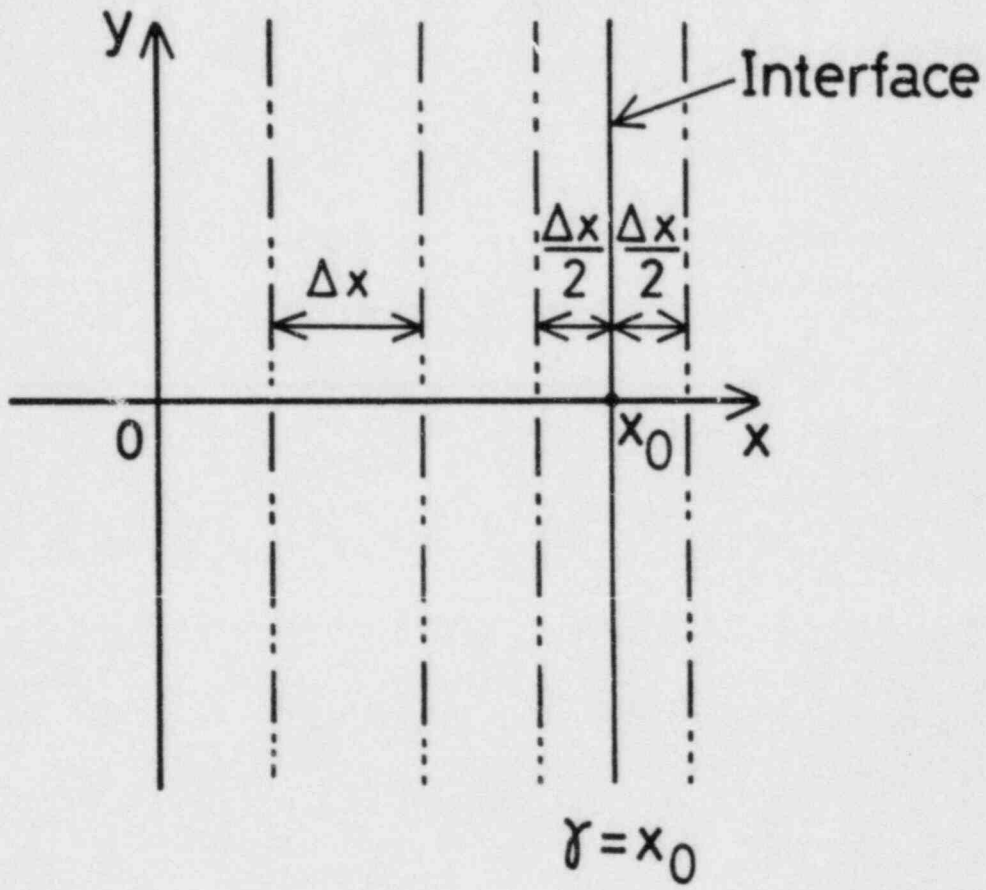

Fig. 1. Local Interfacial Area Concentration in One Dimension

$$\int_{-\infty}^{\infty} \delta(x - x_0)\, \phi(x)dx = \phi(x_0) \tag{15}$$

This result can be extended to any gas-liquid interface in a three dimensional space. By considering a moving gas-liquid interface which is smooth and represented by

$$f(x,y,z,t) = 0 \ , \tag{16}$$

the local instantaneous interfacial area concentration is given by

$$a_i(x,y,z,t) = |\vec{\text{grad}}\ f|\ \delta(f(x,y,z,t)) \tag{17}$$

where $|\vec{\text{grad}}\ f|$ is defined as

$$|\vec{\text{grad}}\ f| = \sqrt{\vec{\text{grad}}\ f \cdot \vec{\text{grad}}\ f} = \sqrt{\left(\frac{\partial f}{\partial x}\right)^2 + \left(\frac{\partial f}{\partial y}\right)^2 + \left(\frac{\partial f}{\partial z}\right)^2} \tag{18}$$

In bubbly or droplet flow, the gas-liquid interface is composed of many separate surfaces of bubbles or droplets. For this case, the surface of the jth bubble or droplet is represented by

$$f_j(x,y,z,t) = 0 \tag{19}$$

Then the local instantaneous interfacial area concentration is given by

$$a_i(x,y,z,t) = \sum_j |\vec{\text{grad}}\ f_j|\ \delta(f_j(x,y,z,t)) \tag{20}$$

The above analysis shows that the local instantaneous formulations of interfacial area concentration can be obtained in terms of a distribution, as in Eq. (20). This formulation is valid for any flow regime of two-phase flow.

Since the distribution, $\delta(x - x_0)$, is not observable experimentally, it is necessary to apply appropriate averaging of Eq. (17) or Eq. (20) to obtain

a measurable representation of the interfacial area concentration. Time and spatial averaging will be discussed in this relation in the next section.

A. Spatial Averaging of Interfacial Area

In general, there are three types of spatial averaging of $a_i(x,y,z,t)$, which are linear, surface, and volume averaging. These are given below.

Linear Average

$$\bar{a}_i^{p1} = \frac{\int_s a_i(x,y,z,t)ds}{\int_s ds} \tag{21}$$

$$dx = ds\ \cos\theta_x$$
$$dy = ds\ \cos\theta_y$$
$$dz = ds\ \cos\theta_z$$

$(\cos\theta_x, \cos\theta_y, \cos\theta_z)$; direction cosines of ds

Surface Average

$$\bar{a}_i^{p2} = \frac{\iint_S a_i(x,y,z,t)dS}{\iint_S dS} \tag{22}$$

$$dydz = dS\ \cos\theta_x$$
$$dzdx = dS\ \cos\theta_y$$
$$dxdy = dS\ \cos\theta_z$$

$(\cos\theta_x, \cos\theta_y, \cos\theta_z)$; direction cosines of the normal vector of dS

Volume Average

$$\bar{a}_i^{p3} = \frac{\iiint_V a_i(x,y,z,t)dV}{\iiint_V dV} \tag{23}$$

$$dV = dxdydz$$

Now, in view of its practical importance for the present study, the linear averaging along z axis is discussed in detail. For fixed x_o, y_o, and t_o, the spatial average of Eq. (20) is given by

$$\bar{a}_i^{pz}(x_o,y_o,t_o) = \frac{1}{L}\int_Z^{Z+L} a_i(x_o,y_o,z,t_o)dz$$

$$= \frac{1}{L}\sum_j \int_Z^{Z+L} |\vec{grad}\ f_j|\ \delta(f_j(x_o,y_o,z,t_o))dz \qquad (24)$$

By defining z_j as the value which satisfies

$$f_j(x_o,y_o,z_j,t_o) = 0 \qquad (25)$$

Equation (24) can be rewritten as

$$\bar{a}_i^{pz}(x_o,y_o,t_o) = \frac{1}{L}\sum_j \left\{|\vec{grad}\ f_j| \Big/ \left|\frac{\partial f_j}{\partial z}\right|\right\} \qquad (26)$$

Here the right hand side is calculated at (x_o,y_o,z_j,t_o) and for jth interface satisfying $z < z_j < z + L$. By denoting the angle between z axis and the direction of the jth surface normal vector at (x_o,y_o,z_j,t_o) as θ_j (see Fig. 2), it can be shown that

$$\cos\theta_j = \left|\frac{\partial f_j}{\partial z}\right| \Big/ |\vec{grad}\ f_j| \qquad (27)$$

Therefore, Eq. (26) becomes

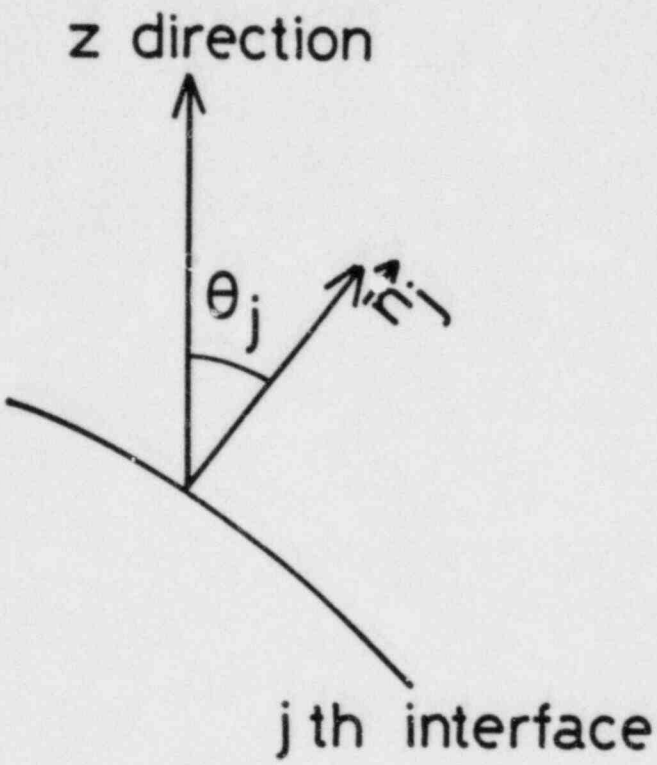

Fig. 2. Angle Between $\vec{n}_z$ (z Direction) and $\vec{n}_j$

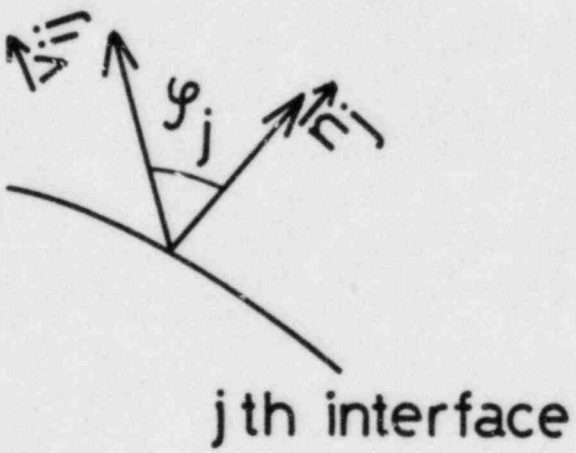

Fig. 3. Angle Between $\vec{v}_{ij}$ and $\vec{n}_j$

$$\bar{a}_i^{pz}(x_o, y_o, t_o) = \frac{1}{L}\sum_j \frac{1}{\cos\theta_j} = \frac{\left(\sum_j\right)}{L}\left\{\sum_j \frac{1}{\cos\theta_j}\Big/\left(\sum_j\right)\right\} \tag{28}$$

Here j is arranged such that z_j is in an increasing order

$$z < \ldots z_{j-1} < z_j < z_{j+1} \ldots < z + L \tag{29}$$

Furthermore, it is asumed that the following uniformity of the two-phase flow exists in the z direction for a reasonably large number of samples.

$$\lim_{n\to\infty} \frac{1}{2n+1} \sum_{j=-n}^{n} |z_{j+1} - z_j| = \ell \tag{30}$$

Then it can be shown that for large L,

$$\left(\sum_j\right) = L/\ell \tag{31}$$

Substituting Eq. (31) into Eq. (28), one finally obtains

$$\bar{a}_i^{pz}(x_o, y_o, t_o) = \frac{1}{\ell}\,\overline{(1/\cos\theta)} \tag{32}$$

Here $\overline{(1/\cos\theta)}$ is the reciprocal of a harmonic mean of $\cos\theta_j$ given by

$$\overline{(1/\cos\theta)} = \left\{\sum_j \frac{1}{\cos\theta_j}\right\}\Big/\left(\sum_j\right) \tag{33}$$

On the other hand, by denoting the number of bubbles or droplets per unit length of z axis by N_Z, ℓ can be given by

$$\ell = \frac{1}{2N_Z} \tag{34}$$

Here the factor 2 indicates that bubble or droplet has two interfaces (upper and lower) in z direction. Then Eq. (32) can be rewritten as

$$\bar{a}_i^{pz}\ (x_o, y_o, t_o) = 2\ N_Z\ \overline{(1/\cos\theta)} \tag{35}$$

Equation (35) implies that the interfacial area concentration can be obtained by measuring the number of bubbles or droplets per unit length and the harmonic average of $\cos\theta_j$ along z direction. If θ_j is not known, one can estimate $\overline{(1/\cos\theta)}$ by assuming certain statistical characteristics of two-phase flow. For a large number of interfaces, Eq. (33) can be approximated by an integral form given by

$$\overline{(1/\cos\theta)} = \int_o^{\pi/2} \frac{p(\theta)}{\cos\theta}\, d\theta \tag{36}$$

where $p(\theta)$ is the probability density function of θ between θ and $\theta + d\theta$. If one assumes that the bubbles or droplets are sphere and every part of sphere is intersected by z axis with equal probability, $p(\theta)$ can be given by

$$p(\theta) = 2\cos\theta\sin\theta \tag{37}$$

Then by substituting Eq. (37) into Eq. (36),

$$\overline{(1/\cos\theta)} = \int_o^{\pi/2} \frac{2\cos\theta\sin\theta}{\cos\theta}\, d\theta = 2 \tag{38}$$

In this case, $\bar{a}_i^{pz}$ is given by the following simple form,

$$\bar{a}_i^{pz}(x_o,y_o,t_o) = 4\,N_Z \tag{39}$$

B. Time Averaging of Interfacial Area

For fixed x_o, y_o, and z_o, the time averaging of Eq. (20) is given by

$$\bar{a}_i^{t}(x_o,y_o,z_o) = \frac{1}{\Omega}\int_T^{T+\Omega} a_i(x_o,y_o,z_o,t)dt = \frac{1}{\Omega}\sum_j \int_T^{T+\Omega} |\vec{\text{grad}}\, f_j|\,\delta(f_j)dt \tag{40}$$

Now t_j is defined as the time which satisfies

$$f_j(x_o,y_o,z_o,t_j) = 0 \tag{41}$$

Then Eq. (40) can be rewritten as

$$\bar{a}_i^{t}(x_o,y_o,z_o) = \frac{1}{\Omega}\sum_j \left\{|\vec{\text{grad}}\, f_j|/\left|\frac{\partial f_j}{\partial t}\right|\right\} \text{ at } (x_o,y_o,z_o,t_j) \tag{42}$$

which applies for j satisfying $T < t_j < T + \Omega$.

By defining ϕ_j as the angle between the velocity of the jth interface, $\vec{v}_{ij}$, and the direction of the surface normal vector at (x_o,y_o,z_o,t_j) (see Fig. 3), the following relation can be obtained

$$|\vec{\text{grad}}\, f_j|/\left|\frac{\partial f_j}{\partial t}\right| = \frac{1}{|\vec{v}_{ij}|\cos\phi_j} \tag{43}$$

Substituting Eq. (43) into Eq. (42), one gets

$$\bar{a}_i^{t}(x_o,y_o,z_o) = \frac{1}{\Omega}\sum_j \frac{1}{|\vec{v}_{ij}|\cos\phi_j} = \frac{\left(\sum_j\right)}{\Omega}\cdot\left\{\left(\sum_j \frac{1}{|\vec{v}_{ij}|\cos\phi_j}\right)\Big/\left(\sum_j\right)\right\} \tag{44}$$

for all j satisfying $T < t_j < T + \Omega$. The above result has been obtained also by Ishii [4] and Delhaye [47,48] using the integral method.

Now j is rearranged so that t_j is in increasing order as

$$\ldots < t_{j-1} < t_j < t_{j+1} < t_{j+2} < \ldots \tag{45}$$

Then by assuming the following uniformity of the time intervals

$$\lim_{n\to\infty} \frac{1}{2n+1} \sum_{j=-n}^{n} |t_{j+1} - t_j| = \tau \tag{46}$$

one obtains the following relation for large Ω

$$\left(\sum_j\right) = \Omega/\tau \tag{47}$$

Substituting Eq. (47) into Eq. (44) yields

$$\bar{a}_i^t (x_o, y_o, z_o) = \frac{1}{\tau} \overline{\frac{1}{|\vec{v}_i| \cos\phi}} \tag{48}$$

Here the reciprocal of a harmonic mean of $|v_{ij}|\cos\phi_j$ is given by

$$\overline{\frac{1}{|\vec{v}_i| \cos\phi}} \cdot \sum_j \frac{1}{|\vec{v}_{ij}| \cos\phi_j} \Big/ \left(\sum_j\right) \tag{49}$$

Now the number of bubbles or droplets which pass the point (x_o, y_o, z_o) per unit time is denoted by N_t, then τ can be given by

$$\tau = \frac{1}{2N_t} \tag{50}$$

Here the factor 2 indicates that one bubble or droplet passing (x_o,y_o,z_o) has two interfaces associated with it. Thus, Eq. (48) can be rewritten by

$$\bar{a}_i^t\,(x_o,y_o,z_o) = 2N_t\,\overline{\frac{1}{|\vec{v}_i|\cos\phi}} \tag{51}$$

This equation indicates that the time-averaged interfacial area concentration can be obtained by counting N_t and knowing $|\vec{v}_{ij}|\cos\phi_j$ for each interface.

If one assumes that $\frac{1}{|\vec{v}_{ij}|}$ and $\frac{1}{\cos\phi_j}$ has no correlation, one obtains (see Appendix A)

$$\overline{\frac{1}{|\vec{v}_i|\cos\phi}} = \overline{\frac{1}{|\vec{v}_i|}} \cdot \overline{\frac{1}{\cos\phi}} \tag{52}$$

where

$$\overline{\frac{1}{|\vec{v}_i|}} = \sum_j \frac{1}{|\vec{v}_{ij}|} \Big/ \left(\sum_j\right) \tag{53}$$

and

$$\overline{\frac{1}{\cos\phi}} = \sum_j \frac{1}{\cos\phi_j} \Big/ \left(\sum_j\right) \tag{54}$$

Then by substituting Eq. (52) into Eq. (51), it can be shown that

$$\bar{a}_i^t\,(x_o,y_o,z_o) = 2N_t\,\overline{\frac{1}{|\vec{v}_i|}} \cdot \overline{\frac{1}{\cos\phi}} \tag{55}$$

C. Ergodic Hypothesis of Interfacial Area Concentration

In the previous sections, spatial and time averaging of the interfacial area concentration has been discussed. However, there is one interesting and practically important problem to consider. This is related to the ergodic hypothesis. It is essential to know under what conditions, the time and spatial averages coincide. A general answer to this problem is quite difficult to obtain and beyond the scope of this report. However, for stationary and developed two-phase flow this ergodic hypothesis can be demonstrated as shown below.

First, the integration of $a_i(x,y,z,t)$ in volume domain V and time domain Ω is considered. This is given by

$$I(V,\Omega) = \iiint_{V,\Omega} a_i(x,y,z,t)dxdydzdt \tag{56}$$

This integral represents the total area of interface in the volume domain V and over the time interval Ω. The sequential integration in time domain Ω and volume V coincides with $I(V,\Omega)$, thus

$$\iiint_V \{\int_\Omega a_i(x,y,z,t)dt\}dxdydz$$

$$= \int_\Omega \{\iiint_V a_i(x,y,z,t)dxdydz\}dt \tag{57}$$

The average value of the interfacial area concentration can be obtained by dividing Eq. (57) by $V\Omega$. Then, in view of Eqs. (23) and (40), Eq. (57) can be rewritten as

$$\overline{\overline{a_i}^{p3}}^{t} = \overline{\overline{a_i}^{t}}^{p3} \tag{58}$$

This shows that the volume average of the time averaged local interfacial area concentration is identical to the time average of the volume averaged concentration. This result is similar to that which Delhaye has proved based on the integral method using the Leibnitz rule [47,48]. Equation (58) might be called the overall ergodic theorem. Although Eq. (58) does not require any

statistical assumptions on the characteristic of two-phase flow, its validity is limited to finite volume and time domains. However, this theorem shows a very important relationship between the time and spatial averages. The ergodic theorem indicates that these two averages are consistent and they represent fundamentally similar physical quantities. It is shown below that by introducing some additional conditions, one can obtain the ergodic theorem which is valid locally.

The integration of $a_i(x,y,z,t)$ in the domain of z from Z to Z + L and t from T to T + Ω is defined by

$$I(L,\Omega) = \iint_{L,\Omega} a_i(x,y,z,t)dzdt \tag{59}$$

This integral has an important physical meaning because it represents the area of interface in the domain from Z to Z + L and from T to T + Ω. Now by changing the sequence of integrations,

$$\int_Z^{Z+L} \{\int_T^{T+\Omega} a_i(x,y,z,t)dt\}dz = \int_T^{T+\Omega} \{\int_Z^{Z+L} a_i(x,y,z,t)dz\}dt \tag{60}$$

Thus by dividing Eq. (60) by LΩ one obtains

$$\frac{1}{L}\int_Z^{Z+L} \{\frac{1}{\Omega}\int_T^{T+\Omega} a_i(x,y,z,t)dt\}dz$$

$$= \frac{1}{\Omega}\int_T^{T+\Omega} \{\frac{1}{L}\int_Z^{Z+L} a_i(x,y,z,t)dz\}dt \tag{61}$$

The above equation is a special case of the general ergodic theorem for the interfacial area concentration given by Eq. (58). A ergodic theorem applicable to the local interfacial area concentration can be obtained by considering stationary and developed two-phase flow. For this type of two-phase flow, appropriately averaged two-phase flow parameters are independent of time

and axial location. By applying these characteristics to the interfacial area concentration, the following results can be obtained.

$$\bar{a}_i^t \equiv \frac{1}{\Omega}\int_T^{T+\Omega} a_i(x,y,z,t)dt = A(x,y) \tag{62}$$

and

$$\bar{a}_i^{pz} \equiv \frac{1}{L}\int_Z^{Z+L} a_i(x,y,z,t)dz = B(x,y) \tag{63}$$

where z is the direction of flow. By substituting Eqs. (62) and (63) into Eq. (61) and integrating it, it can be shown that

$$\frac{1}{L}\int_Z^{Z+L} A(x,y)dz = \frac{1}{\Omega}\int_T^{T+\Omega} B(x,y)dt \tag{64}$$

This can be satisfied for arbitrary values of x and y only if

$$A(x,y) = B(x,y) \tag{65}$$

Therefore, for stationary and developed two-phase flow, the linear averaging $\bar{a}_i^{pz}$ and the time averaging $\bar{a}_i^t$ becomes identical when the linear averaging is taken along the flow direction. Thus,

$$\bar{a}_i^{pz} = \bar{a}_i^t \text{ (for stationary and developed flow)} \tag{66}$$

In comparison with the general ergodic theorem given by Eq. (58), Eq. (66) can be called the local ergodic theorem. From Eqs. (32) and (48) this ergodic theorem can be modified to

$$\frac{1}{\ell}\overline{(1/\cos\theta)} = \frac{1}{\tau}\overline{\frac{1}{|\vec{v}_i|\cos\phi}} \tag{67}$$

The local ergodic theorem given by Eq. (66) is quite important in terms of practical applications. This is because the theorem indicates that the line averaged interfacial area concentration can be obtained from the time-averaged local interfacial area concentration. The latter can be related to measurable quantities in a two-phase flow system. For example, the time-averaged local interfacial area concentration can be measured from the number of bubbles or drops and the interfacial velocity as shown in Eq. (51).

III. MEASUREMENT METHOD OF LOCAL INTERFACIAL AREA CONCENTRATION

As discussed in the preceeding sections, there are two possible methods for measuring the local interfacial area concentration. The first approach is to use the principle indicated by Eq. (35). Equations (33) and (34) show that one has to measure the number of bubbles or droplets and a direction cosine of a normal vector of each interface in the sufficiently large z axis distance between Z and Z + L. For this, it is necessary to use a sensor which scans distance L in a negligible time duration. In other words, the sensor velocity must be much larger than the velocity of interfaces. The optical techniques such as a photography or light attenuation method may be applied for this purpose. Several attempts have been made based on these methods [31,39,40]. However, at present, this approach has a limited success only for very low void fraction two-phase flow. At higher void fraction, the light scattering and refraction at multiple interfaces become a very serious problem. Due to these difficulties in the experimental technique, a complete measurement of the local interfacial area concentration based on Eqs. (33), (34), and (35) has not been accomplished yet.

Another approach is to use a principle indicated by Eq. (51). In view of Eqs. (49) and (50), this method requires a sensor located in a fixed point in two-phase flow and being capable of measuring the number of bubbles or droplets, their interfacial velocity and the angle between the interfacial velocity and normal vector of the interface. For this purpose, electrical resistivity probe, optical probe, and anemometer which are often used in two-phase flow measurements [49,50] may be suitable. In what follows, the measurement using an electrical resistivity probe will be discussed in detail.

Figure 4 schematically shows a double-sensored electrical resistivity probe. Sensors 1 and 2 detect gas and liquid phase by means of the difference

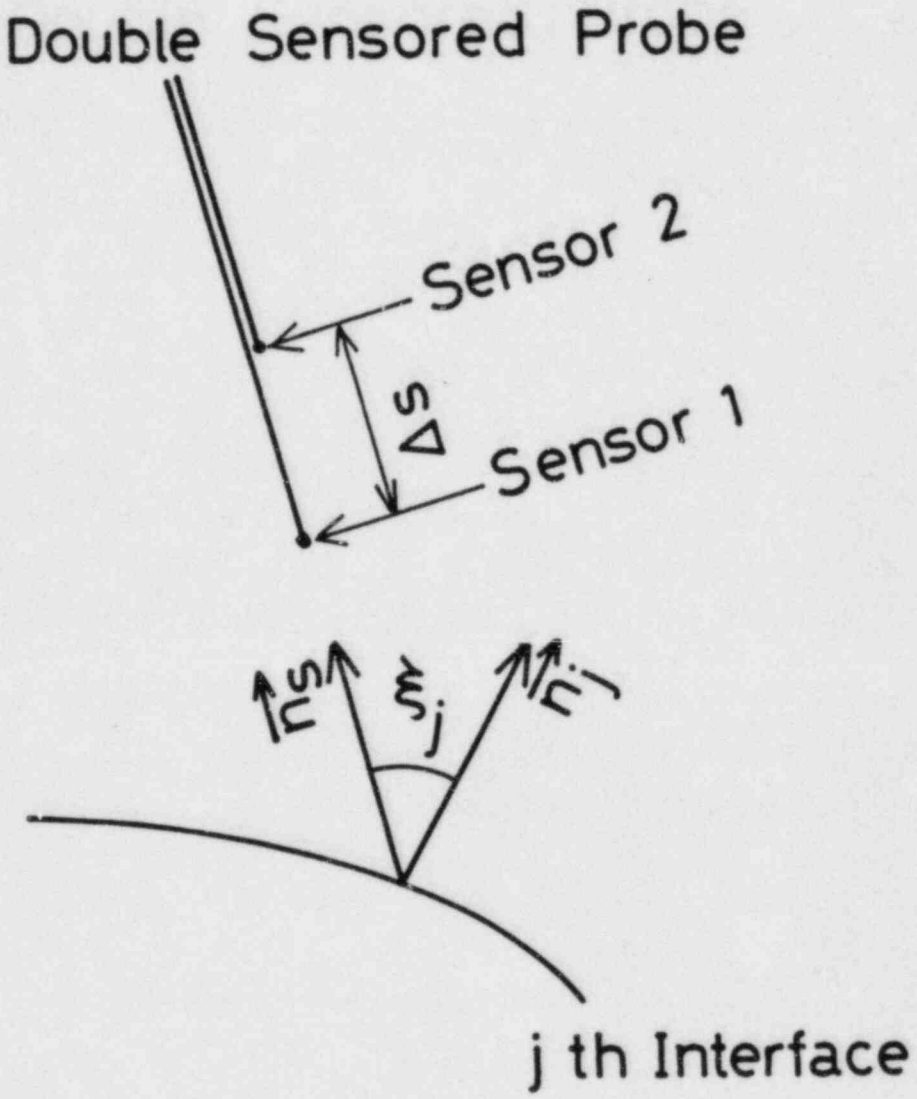

Fig. 4. Double Sensored Probe and jth Interface

between gas and liquid electrical resistivity. Therefore, from the electrical signals out of these sensors, a gas liquid interface can be detected. Therefore, using these sensors, the number of interfaces passing the probe per unit time, N_t, can be measured. Furthermore, by measuring the time difference Δt for an interface to pass sensors 1 and 2, the velocity of interface passing the probe can be measured. Here this velocity is denoted by v_s which is given by

$$v_s = \frac{\Delta s}{\Delta t} \tag{68}$$

Now consider a unit vector, $\vec{n}_s$, which direction is same as that of a double sensored probe (Fig. 4). Its direction cosines are represented by $(\cos n_x, \cos n_y, \cos n_z)$. The position of sensor 1 is given by (x_o, y_o, z_o), then the position of sensor 2 is given by $(x_o+\Delta s\cos n_x, y_o+\Delta s\cos n_y, z_o+\Delta s\cos n_z)$. By considering the jth interface passing the sensors 1 and 2, with the passing velocity of v_{sj} and the interval of Δt_j, the following relation exists.

$$v_{sj} = \frac{\Delta s}{\Delta t_j} \tag{69}$$

Since the jth surface is represented by Eq. (19), the surface equation should satisfy

$$f_j(x_o, y_o, z_o, t_j) = 0 \tag{70}$$

$$f_j(x_o+\Delta s\cos n_x,\ y_o+\Delta s\cos n_y,\ z_o+\Delta s\cos n_z,\ t_j + \Delta t_j) = 0 \tag{71}$$

where t_j is the time when the jth interface passes the sensor 1. When Δs is small, Eqs. (70) and (71) give the following approximate relation

$$\Delta s(\vec{\text{grad}}\ f_j) \cdot \vec{n}_s = -\frac{\partial f_j}{\partial t}\Delta t_j \tag{72}$$

In view of Eq. (69), the above equation can be transformed to

$$v_{sj} = \frac{-\frac{\partial f_j}{\partial t}}{(\vec{\text{grad}}\, f_j) \cdot \vec{n}_s} \tag{73}$$

The angle between $\vec{n}_s$ and $\vec{n}_j$ which is the surface unit normal vector of the jth interface is denoted by ξ_j as shown in Fig. 4, then it can be shown that

$$\vec{n}_j \cdot \vec{n}_s = \cos\xi_j = \frac{(\vec{\text{grad}}\, f_j) \cdot \vec{n}_s}{|\vec{\text{grad}}\, f_j|} \tag{74}$$

From Eqs. (73), (74), and (43),

$$|v_{sj}|\cos\xi_j = |\vec{v}_{ij}|\cos\phi_j \tag{75}$$

On the other hand, Eq. (73) can be rewritten as

$$\frac{\partial f_j}{\partial x}\cos\eta_x + \frac{\partial f_j}{\partial y}\cos\eta_y + \frac{\partial f_j}{\partial z}\cos\eta_z = -\frac{\frac{\partial f_j}{\partial t}}{v_{sj}} \tag{76}$$

Equation (76) indicates that it is possible to calculate the value given by Eq. (75) by using three double-sensored probes with a common sensor. It is schematically shown in Fig. 5. The unit vector and its direction cosines for probe k are represented by $\vec{n}_{sk}$ and $(\cos\eta_{xk}, \cos\eta_{yk}, \cos\eta_{zk})$ with k = 1, 2, 3. The passing velocity of the jth interface over probe k, is denoted by v_{skj}. Then from Eq. (76) one obtains

$$\frac{\partial f_j}{\partial x}\cos\eta_{xk} + \frac{\partial f_j}{\partial y}\cos\eta_{yk} + \frac{\partial f_j}{\partial z}\cos\eta_{zk} = -\frac{\partial f_j}{\partial t}\frac{1}{v_{skj}} \tag{77}$$

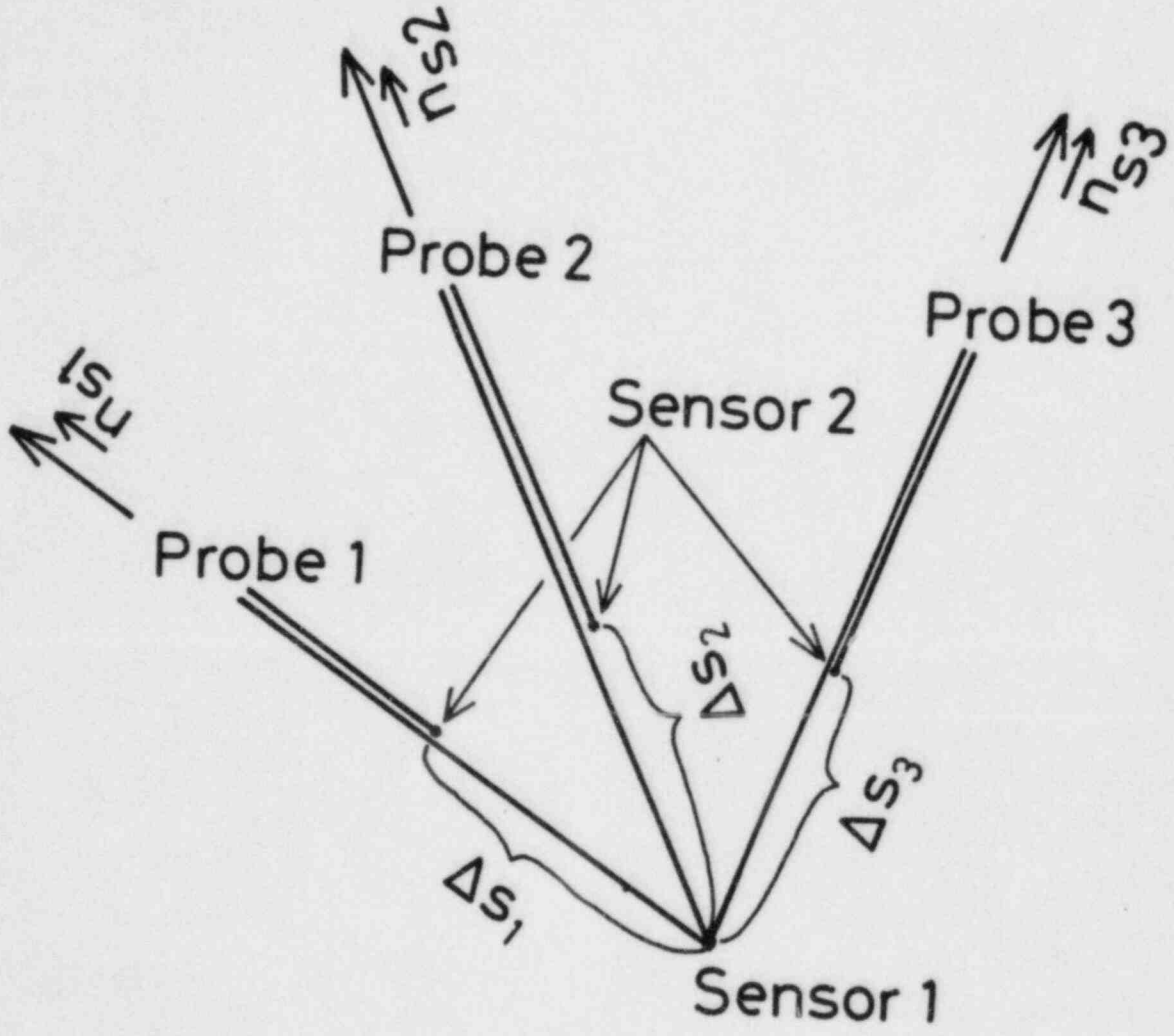

Fig. 5. Three Double Sensored Probes

The directions of three probes can be made independent, then it implies

$$|A_o| \equiv \begin{vmatrix} \cos n_{x1}, & \cos n_{y1}, & \cos n_{z1} \\ \cos n_{x2}, & \cos n_{y2}, & \cos n_{z2} \\ \cos n_{x3}, & \cos n_{y3}, & \cos n_{z3} \end{vmatrix} \neq 0 \tag{78}$$

Under this condition, Eq. (77) has a solution. From this solution, it can be shown that

$$\frac{\left|\frac{\partial f_j}{\partial t}\right|}{|\vec{\text{grad}}\ f_j|} = \frac{\sqrt{|A_o|^2}}{\sqrt{|A_1|^2 + |A_2|^2 + |A_3|^2}} \tag{79}$$

where $|A_1|$, $|A_2|$, and $|A_3|$ are given by

$$|A_1| \equiv \frac{1}{v_{s1j}} \begin{vmatrix} 1, & \cos n_{y1}, & \cos n_{z1} \\ 1, & \cos n_{y2}, & \cos n_{z2} \\ 1, & \cos n_{y3}, & \cos n_{z3} \end{vmatrix} \tag{80}$$

$$|A_2| \equiv \frac{1}{v_{s2j}} \begin{vmatrix} \cos n_{x1}, & 1, & \cos n_{z1} \\ \cos n_{x2}, & 1, & \cos n_{z2} \\ \cos n_{x3}, & 1, & \cos n_{z3} \end{vmatrix} \tag{81}$$

$$|A_3| \equiv \frac{1}{v_{s3j}} \begin{vmatrix} \cos n_{x1}, & \cos n_{y1}, & 1 \\ \cos n_{x2}, & \cos n_{y2}, & 1 \\ \cos n_{x3}, & \cos n_{y3}, & 1 \end{vmatrix} \tag{82}$$

In view of Eq. (43), the above result gives

$$|\vec{v}_{ij}|\cos\phi_j = \frac{\sqrt{|A_1|^2 + |A_2|^2 + |A_3|^2}}{\sqrt{|A_o|^2}} \tag{83}$$

If x, y, and z directions are chosen to be the directions of the three probes, or $\vec{n}_{s1}$, $\vec{n}_{s2}$, and $\vec{n}_{s3}$, Eqs. (78) through (83) gives

$$|\vec{v}_{ij}|\cos\phi_j = \sqrt{\left(\frac{1}{v_{s1j}}\right)^2 + \left(\frac{1}{v_{s2j}}\right)^2 + \left(\frac{1}{v_{s3j}}\right)^2} \tag{84}$$

The the time-averaged local interfacial area concentration can be measured in view of Eqs. (49) and (51) from the following relation.

$$\bar{a}_i^t(x_o, y_o, z_o) = \frac{1}{\tau}\left\{\sum_j \frac{1}{\sqrt{(1/v_{s1j})^2 + (1/v_{s2j})^2 + (1/v_{s3j})^2}}\right\} \Bigg/ \left(\sum_j\right) \tag{85}$$

Although in principle this method gives accurate measurement of an interfacial area concentration, there are some problems in terms of practical applications. In deriving Eq. (72) from Eqs. (70) and (71), it has been assumed that Δs is small. In view of the effect of curvature of bubble or droplet interfaces, the accuracy of the measurement increases as Δs decrease. On the other hand, Eq. (69) indicates that Δt_j decreases with decreasing Δs. This implies that one has to measure smaller Δt_j as Δs decreases. Then the accuracy of measuring Δt_j and that of v_{sj} decreases as Δs becomes smaller. Therefore, in practical measurements, the determination of optimum Δs should be an important problem which requires utmost attention.

The above described method based on the three double-sensored probes may be difficult to apply if the required sensor distance is very small. It is evident that Δs should be considerably smaller than a bubble or drop diameter. Furthermore, deformations of interfaces by the probes should also be carefully examined. It can be said that this method will encounter increasing difficulties as the fluid particle size becomes smaller. In view of the above, a simpler probe method which can be applied to many two-phase conditions is highly desirable. One possibility is to use a single double-sensored probe. However, in this case it becomes necessary to assume certain statistical characteristics of two-phase flow.

Now a double-sensored probe located in z direction is considered where the mean flow is assumed to also be in the z direction. The velocity and the normal unit vector of the jth interface, $\vec{v}_{ij}$ and $\vec{n}_j$, can be given in terms of unit vectors $\vec{n}_x$, $\vec{n}_y$, and $\vec{n}_z$, using angles with z and y axes given by (α_j, β_j) and (μ_j, ν_j) and shown in Figs. 6 and 7. Thus,

$$\vec{v}_{ij} = |\vec{v}_{ij}| \{\cos\alpha_j \, \vec{n}_z + \sin\alpha_j \cos\beta_j \, \vec{n}_y + \sin\alpha_j \sin\beta_j \, \vec{n}_x\} \tag{86}$$

$$\vec{n}_j = \cos\mu_j \, \vec{n}_z + \sin\mu_j \cos\nu_j \, \vec{n}_y + \sin\mu_j \sin\nu_j \, \vec{n}_x \tag{87}$$

Then it can be shown that

$$|\vec{v}_{ij}| \cos\phi_j = \vec{v}_{ij} \cdot \vec{n}_j$$

$$= |\vec{v}_{ij}| \{\cos\alpha_j \cos\mu_j + \sin\alpha_j \sin\mu_j \cos(\beta_j - \nu_j)\} \tag{88}$$

Substituting Eq. (88) into Eq. (49) one obtains

$$\overline{\frac{1}{|\vec{v}_i|\cos\phi}} = \sum_j \frac{1}{|\vec{v}_{ij}| \{\cos\alpha_j \cos\mu_j + \sin\alpha_j \sin\mu_j \cos(\beta_j - \nu_j)\}} \Bigg/ \left(\sum_j\right) \tag{89}$$

By assuming that there are no statistical correlations between $|\vec{v}_{ij}|$ and ϕ_j (randomness of $\vec{v}_{ij}$), Eq. (52) can be used. Then in view of Eq. (89),

$$\overline{\frac{1}{|\vec{v}_i|\cos\phi}} = \sum_j \frac{1}{|\vec{v}_{ij}|} \Bigg/ \left(\sum_j\right)$$

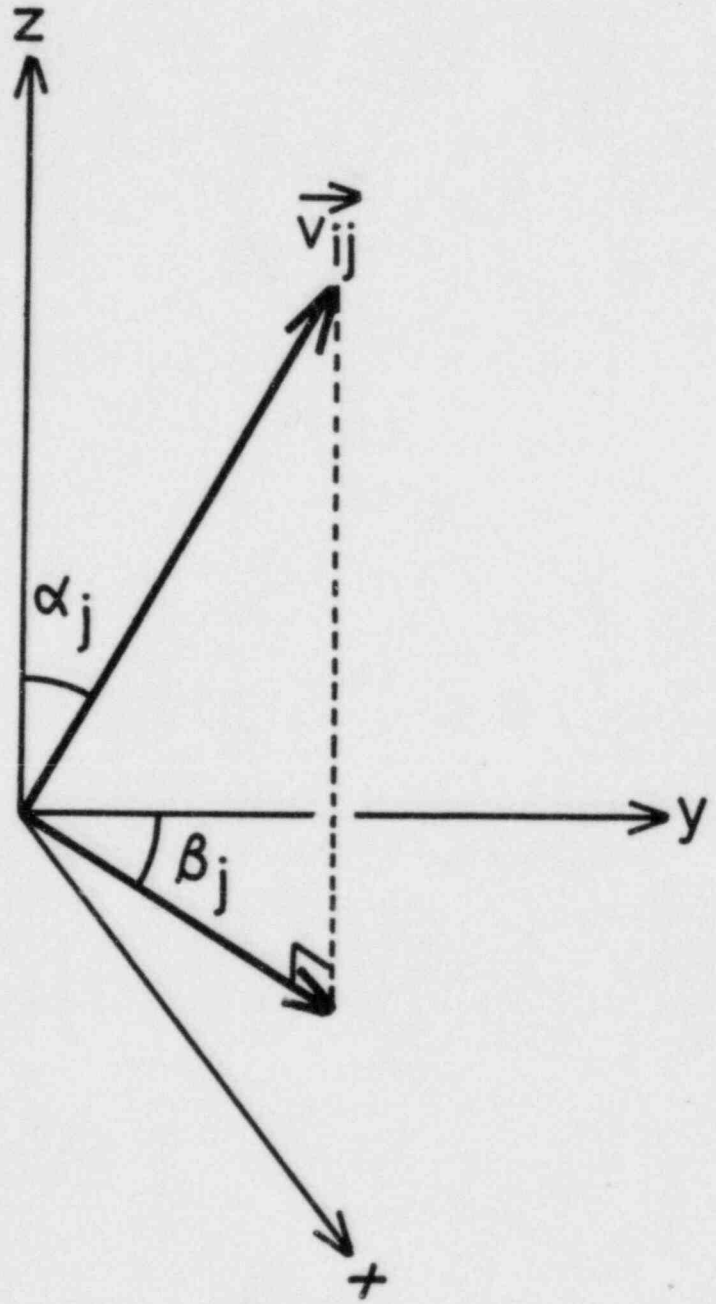

Fig. 6. Angles α_j and β_j for $\vec{v}_{ij}$

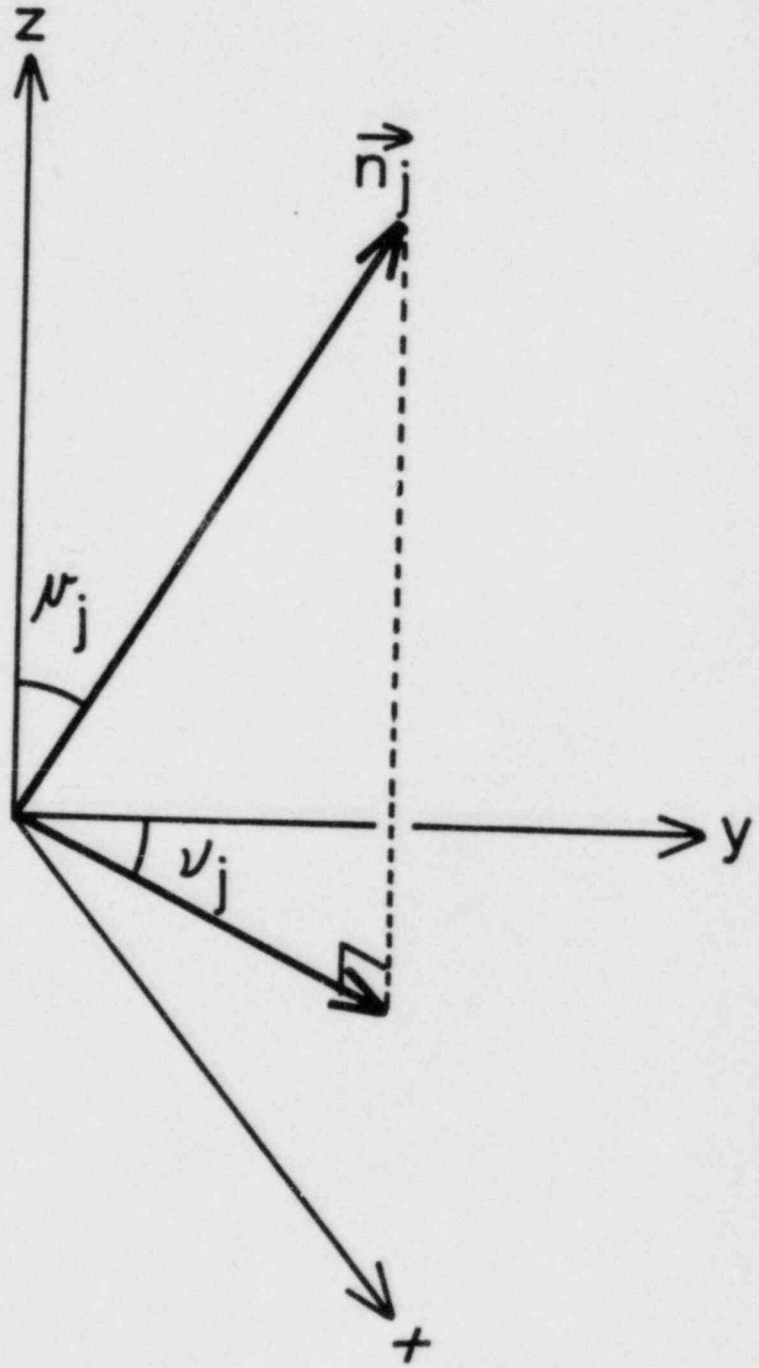

Fig. 7. Angles μ_j and ν_j for $\vec{n}_j$

$$\times \left[\sum_j \frac{1}{\{\cos\alpha_j \cos\mu_j + \sin\alpha_j \sin\mu_j \cos(\beta_j - \nu_j)\}} \right] \Bigg/ \left(\sum_j \right) \tag{90}$$

When the number of measured interfaces is large, the summation can be approximated by an integration. Thus,

$$\sum_j \frac{1}{\{\cos\alpha_j \cos\mu_j + \sin\alpha_j \sin\mu_j \cos(\beta_j - \nu_j)\}} \Bigg/ \left(\sum_j \right)$$

$$\doteq \iint_{\alpha,\mu=0}^{\pi/2} \iint_{\beta,\nu=0}^{2\pi} \frac{P(\alpha,\beta,\mu,\nu)}{\{\cos\alpha \cos\mu + \sin\alpha \sin\mu \cos(\beta - \nu)\}} d\alpha d\beta d\mu d\nu \tag{91}$$

where $P(\alpha,\beta,\mu,\nu)$ is a probability density function of α, β, μ, ν. Then Eq. (90) can be rewritten as

$$\overline{\frac{1}{|\vec{v}_i|\cos\phi}} = \left\{ \sum_j \frac{1}{|\vec{v}_{ij}|} \Bigg/ \left(\sum_j \right) \right\} \cdot \iiiint \frac{P(\alpha,\beta,\mu,\nu) d\alpha d\beta d\mu d\nu}{\{\cos\alpha \cos\mu + \sin\alpha \sin\mu \cos(\beta-\nu)\}} \tag{92}$$

On the other hand, in view of Eq. (75), the measured velocity v_{sz} associated with the jth interface passing the double-sensored probe located in z direction is given by

$$|v_{szj}| \cos\xi_j = |\vec{v}_{ij}| \cos\phi_j \tag{93}$$

Since the probe direction is in the z direction,

$$\vec{n}_s = \vec{n}_z \tag{94}$$

Substituting Eqs. (87) and (94) into Eq. (74), one gets

$$\cos\xi_j = \cos\mu_j \tag{95}$$

In view of Eqs. (93) and (95) and assuming that no statistical correlation exists between $|\vec{v}_{ij}|$ and μ_j, it can be shown

$$\sum_j \frac{1}{|v_{szj}|} \Big/ \left(\sum_j\right) \doteq \left\{\sum_j \frac{1}{|\vec{v}_{ij}|} \Big/ \left(\sum_j\right)\right\} \iiiint \frac{P(\alpha,\beta,\mu,\nu)\cos\mu \, d\alpha d\beta d\mu d\nu}{\{\cos\alpha\cos\mu + \sin\alpha\sin\mu\cos(\beta-\nu)\}} \quad (96)$$

where $0 \leq \alpha, \mu \leq \pi/2$, and $0 \leq \beta, \nu \leq 2\pi$.

In view of Eqs. (92), (96), and (48), the time-averaged local interfacial area concentration is given in terms of the measured velocities of interfaces and the probability density function. Hence

$$\bar{a}_i^t (x_o, y_o, z_o) = \frac{1}{\tau}\left\{\sum_j \frac{1}{|v_{szj}|} \Big/ \left(\sum_j\right)\right\}$$

$$\times \iiiint \frac{P(\alpha,\beta,\mu,\nu) d\alpha d\beta d\mu d\nu}{\{\cos\alpha\cos\mu + \sin\alpha\sin\mu\cos(\beta-\nu)\}}$$

$$/ \iiiint \frac{P(\alpha,\beta,\mu,\nu)\cos\mu \, d\alpha d\beta d\mu d\nu}{\{\cos\alpha\cos\mu + \sin\alpha\sin\mu\cos(\beta-\nu)\}} \quad (97)$$

Equation (97) indicates that $\bar{a}_i^t$ can be calculated from measured values of the bubble or droplet number, N_t, and of the passing velocities of interfaces using one double-sensored probe. However, in addition to these it is necessary to assume a form of the probability density function, $P(\alpha,\beta,\mu,\nu)$. For this purpose, it is assumed that the interfaces are composed of spherical bubbles or droplets and the probe passes every part of bubble or droplet with an equal probability. Furthermore, it is assumed that the x and y direction components of $\vec{v}_{ij}$ is random. Under these assumptions, β and ν takes any value between 0 and 2π with equal probability and β and ν are statistically independent of each other. Then the probability density function can be reduced to

$$P(\alpha,\beta,\mu,\nu)d\alpha d\beta d\mu d\nu = P(\alpha,\mu,(\beta-\nu))d\alpha d\mu d(\beta-\nu)$$

$$= \frac{1}{\pi} g(\alpha)\sin\mu\cos\mu\, d\alpha d\mu d(\beta-\nu) \tag{98}$$

By substituting Eq. (98) into Eq. (97) and in view of Eq. (50), one finally obtains the following result after carrying out the integration

$$\bar{a}_i^t(x_o,y_o,z_o) = 4N_t\left\{\sum_j \frac{1}{|v_{szj}|}\Big/\left(\sum_j\right)\right\}$$

$$\times \frac{1}{1 + \dfrac{\int_0^{\pi/2} g(\alpha)\sin\alpha\, \ell n\left(\dfrac{1+\cos\alpha}{\sin\alpha}\right) d\alpha}{\int_0^{\pi/2} g(\alpha)\cos\alpha\, d\alpha}} \tag{99}$$

Since the main flow is in the z direction, the major component of the interfacial velocity is also the z component, if the mean flow velocity is not small compared with the fluctuating x and y components. In that case, $g(\alpha)$ is considered to have a sharp peak at $\alpha = 0$. Hence as a first approximation, $g(\alpha)$ may be represented by a delta function as

$$g(\alpha) = \delta(\alpha) \tag{100}$$

Then Eq. (99) can be simplified to

$$\bar{a}_i^t(x_o,y_o,z_o) = 4N_t\left\{\sum_j \frac{1}{|v_{szj}|}\Big/\left(\sum_j\right)\right\} = 4N_t\,\overline{\frac{1}{|v_{sz}|}} \tag{101}$$

The approximation given by Eq. (100) implies that the interfacial velocity $\vec{v}_{ij}$ has only the z component. Equation (101) has also been obtained by Sekoguchi [51-53] and Herringe et al. [54] based on the bubble diameter distribution assuming spherical bubble.

A more accurate approximation for $f(\alpha)$ may be given by

$$g(\alpha) = \frac{1}{\alpha_o} \quad \text{for } 0 \leq \alpha < \alpha_o$$

$$= 0 \quad \text{for } \alpha_o < \alpha < \frac{\pi}{2} \tag{102}$$

This form of $g(\alpha)$ implies that the angle α made by the interfacial velocity and the z axis is random with an equal probability within the maximum angle of α_o. Substituting Eq. (102) into Eq. (99), the interfacial area concentration becomes

$$\bar{a}_i^t (x_o, y_o, z_o) = \frac{4 N_t \left\{ \sum_j \frac{1}{|v_{szj}|} \Big/ \left(\sum_j \right) \right\}}{1 - \cot \frac{\alpha_o}{2} \ln \left(\cos \frac{\alpha_o}{2} \right) - \tan \frac{\alpha_o}{2} \ln \left(\sin \frac{\alpha_o}{2} \right)} \tag{103}$$

Therefore, by knowing the value of α_o, the time-averaged local interfacial area concentration can be calculated from the measured values of N_t and v_{szj}. α_o can be estimated from measured values of statistical parameters of interfacial velocity as explained below.

As shown in Eq. (86), $\vec{v}_{ij}$ is composed of x, y, and z components, $\vec{v}_{ixj}$, $\vec{v}_{iyj}$, and $\vec{v}_{izj}$, which are given by

$$\vec{v}_{ixj} = |\vec{v}_{ij}| \sin\alpha_j \sin\beta_j \vec{n}_x \tag{104}$$

$$\vec{v}_{iyj} = |\vec{v}_{ij}| \sin\alpha_j \cos\beta_j \vec{n}_y \tag{105}$$

$$\vec{v}_{izj} = |\vec{v}_{ij}| \cos\alpha_j \vec{n}_z \tag{106}$$

They should satisfy

$$\vec{v}_{ij} = \vec{v}_{ixj} + \vec{v}_{iyj} + \vec{v}_{izj} \tag{107}$$

If there is no prefered direction for an instantaneous transverse velocity, β has a probability density function given by

$$h(\beta) = \frac{1}{2\pi} \quad , \quad 0 \leq \beta \leq 2\pi \tag{108}$$

Then in view of Eq. (86) with the assumption for $g(\alpha)$ given by Eq. (102), one gets

$$\overline{\vec{v}_{ix}} = \left(\sum_j \vec{v}_{ixj}\right) \Big/ \left(\sum_j\right)$$

$$= \overline{|\vec{v}_i|} \int_0^{\pi/2} g(\alpha)\sin\alpha d\alpha \int_0^{2\pi} h(\beta)\sin\beta d\beta \cdot \vec{n}_x$$

$$= 0 \tag{109}$$

Similarly,

$$\overline{\vec{v}_{iy}} = 0 \tag{110}$$

On the other hand,

$$\overline{\vec{v}_{iz}} = \overline{|\vec{v}_i|} \int_0^{\pi/2} g(\alpha)\cos\alpha d\alpha \cdot \vec{n}_z = \overline{|\vec{v}_i|} \frac{\sin\alpha_0}{\alpha_0} \vec{n}_z \tag{111}$$

Here no statistical correlations between $|\vec{v}_{ij}|$, α, and β has been assumed.

The mean squares of velocity fluctuations are given by the following expressions. For the x components,

$$\sigma_x^2 \equiv \overline{(\vec{v}_{ix} - \overline{\vec{v}_{ix}})^2} = \overline{|\vec{v}_{ix}|^2} - |\overline{\vec{v}_{ix}}|^2 = \overline{|\vec{v}_{ix}|^2}$$

$$= \overline{|\vec{v}_i|^2} \int_0^{\pi/2} g(\alpha)\sin^2\alpha d\alpha \int_0^{2\pi} h(\beta)\sin^2\beta d\beta$$

$$= \frac{1}{2}\overline{|\vec{v}_i|^2}\left\{\frac{1}{2} - \frac{1}{4}\frac{\sin 2\alpha_0}{\alpha_0}\right\} \tag{112}$$

for the y components,

$$\sigma_y^2 \equiv \overline{(\vec{v}_{iy} - \overline{\vec{v}_{iy}})^2} = \overline{|\vec{v}_{iy}|^2} = \frac{1}{2}\overline{|\vec{v}_i|^2}\left\{\frac{1}{2} - \frac{1}{4}\frac{\sin 2\alpha_0}{\alpha_0}\right\} = \sigma_x^2 \tag{113}$$

and for the z component,

$$\sigma_z^2 \equiv \overline{(\vec{v}_{iz} - \overline{\vec{v}_{iz}})^2} = \overline{|\vec{v}_{iz}|^2} - |\overline{\vec{v}_{iz}}|^2 = \overline{|\vec{v}_i|^2} \int_0^{\pi/2} g(\alpha)\cos^2\alpha d\alpha - |\overline{\vec{v}_{iz}}|^2$$

$$= \overline{|\vec{v}_i|^2}\left\{\frac{1}{2} + \frac{1}{4}\frac{\sin 2\alpha_0}{\alpha_0}\right\} - |\overline{\vec{v}_{iz}}|^2 \tag{114}$$

On the other hand, from Eq. (101),

$$\overline{|\vec{v}_i|^2} = \overline{|\vec{v}_{ix}|^2} + \overline{|\vec{v}_{iy}|^2} + \overline{|\vec{v}_{iz}|^2} \tag{115}$$

Furthermore, from an assumption that the velocity fluctuations are equilateral,

$$\sigma_x^2 = \sigma_y^2 = \sigma_z^2 \tag{116}$$

Then combining the above results given by Eqs. (112) to (116), it can be shown

$$\frac{\sin 2\alpha_o}{2\alpha_o} = \frac{1 - (\sigma_z^2 / \overline{|\vec{v}_{iz}|^2})}{1 + 3\,(\sigma_z^2 / \overline{|\vec{v}_{iz}|^2})} \tag{117}$$

Thus by knowing the mean value and fluctuations of z component interfacial velocity, it is possible to estimate the value of α_o.

IV. EXPERIMENTAL VALUE OF LOCAL INTERFACIAL AREA CONCENTRATION

As shown in the previous section, the time-averaged local interfacial area concentration can be calculated from measured values of the bubble or droplet number per unit time and mean and fluctuating components of the interfacial velocity using Eqs. (103) and (117).

Serizawa et al. [55-58], have measured the above mentioned parameters in air-water bubbly and slug flow in a vertical tube. Under stationary and developed conditions, they measured the bubble number per unit time, N_t and spectrum of passing velocity of interface, $|v_{sz}|$ at various radial positions. The examples of the spectra of $|v_{sz}|$ are shown in Fig. 8. From these spectra, one can calculate the reciprocal of a harmonic mean of $|v_{sz}|$ as

$$\overline{\frac{1}{|v_{sz}|}} = \left\{ \sum_j \frac{1}{|v_{szj}|} \Big/ \left(\sum_j \right) \right\} = \int_o^\infty \frac{w(|v_{sz}|)}{|v_{sz}|}\, d|v_{sz}| \tag{118}$$

where $w(|v_{sz}|)$ is the probability density function of $|v_{sz}|$ corresponding to the normalized spectrum shown in Fig. 8. Similarly, the square mean of the fluctuation of $|v_{sz}|$ can be calculated from the spectra as

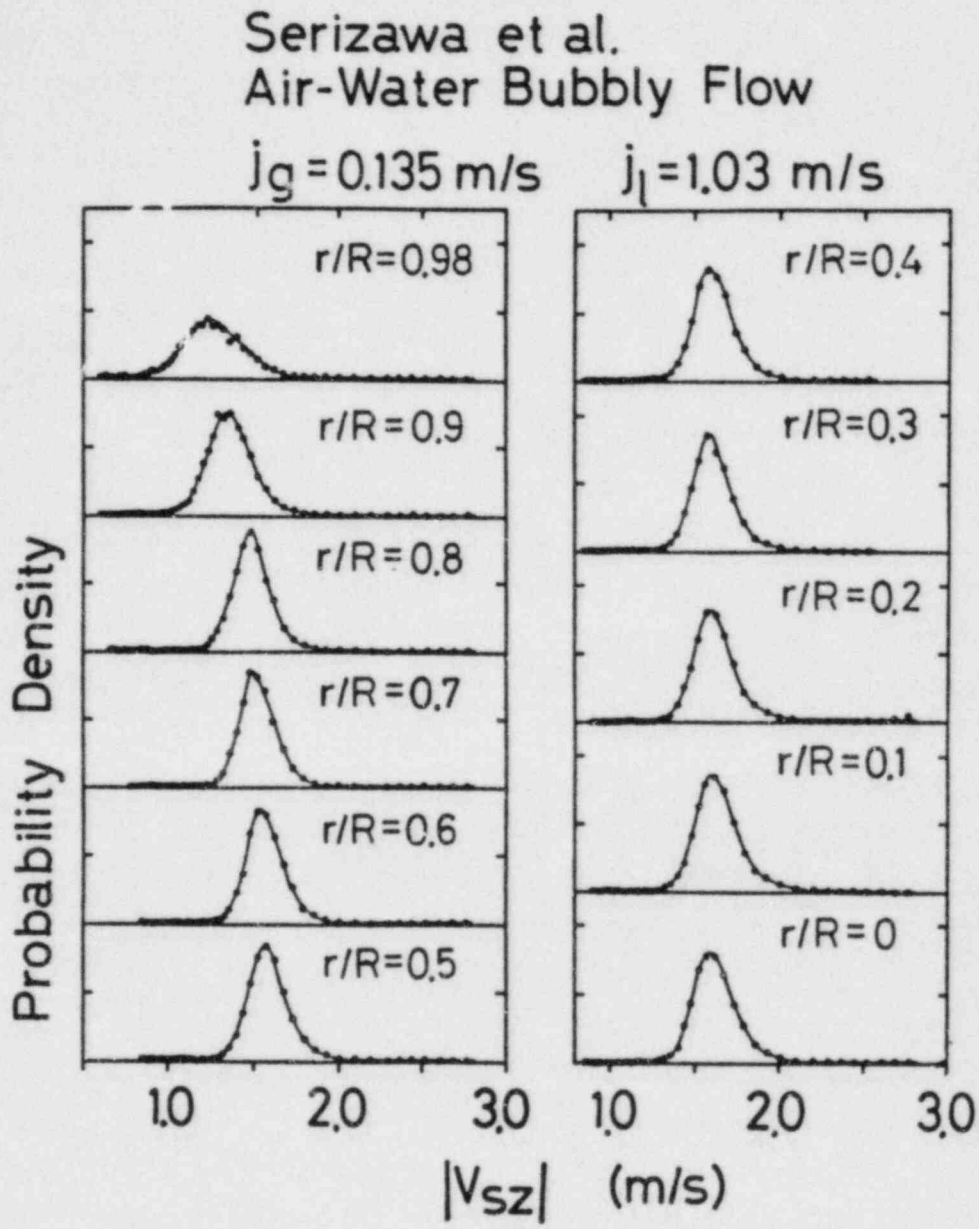

Fig. 8. Spectra of $|v_{sz}|$ for Air-Water Bubbly Flow at j_g = 0.135 m/s and j_ℓ = 1.03 m/s at Various Radial Positions (Serizawa et al. [55,57])

$$\sigma_{sz}^2 = \left\{ \sum_j (|v_{szj}| - \overline{|v_{sz}|})^2 \Big/ \left(\sum_j \right) \right\}$$

$$= \int_0^\infty |v_{sz}|^2 \, w(|v_{sz}|) \, d|v_{sz}| - \{ \int_0^\infty |v_{sz}| \, w(|v_{sz}|) \, d|v_{sz}| \}^2 \qquad (119)$$

where

$$\overline{|v_{sz}|} = \int_0^\infty |v_{sz}| \, w(|v_{sz}|) \, d|v_{sz}| \qquad (120)$$

The value of $\sigma_z^2 / \overline{|\vec{v}_{iz}|}^2$ is not measured in Serizawa's experiment. However, one can approximate this value as

$$\frac{\sigma_z^2}{\overline{|\vec{v}_{iz}|}^2} \simeq \frac{\sigma_{sz}^2}{\overline{|v_{sz}|}^2} \qquad (121)$$

which is calculated by Eqs. (119) and (120) from the measured spectrum of $|v_{sz}|$. Figure 9 shows one example of the profiles of N_t, $1/\overline{(1/|v_{sz}|)}$, and $\sigma_{sz}/\overline{|v_{sz}|}$ calculated from the above procedure. Thus one obtains the local interfacial area concentration from Eqs. (103) and (117) using the measured values of N_t and spectrum of $|v_{sz}|$.

Figures 10 to 15 show the local interfacial area concentration profiles based on the above-described method and the experimental data of Serizawa et al. [55-58]. In the figures, r denotes a radial position and R denotes radius of flow passage. For bubbly flow the local interfacial area concentration shows rather uniform values in the center region of the tube and higher values near the tube wall. The higher values suggest that in this type of bubbly flow the interfacial transport of momentum and heat is higher near the tube wall. On the other hand, in slug flow and bubbly to slug transition flows the local interfacial area concentration does not show an appreciable peak value near the tube wall as indicated in Figs. 14 and 15. However, higher values of

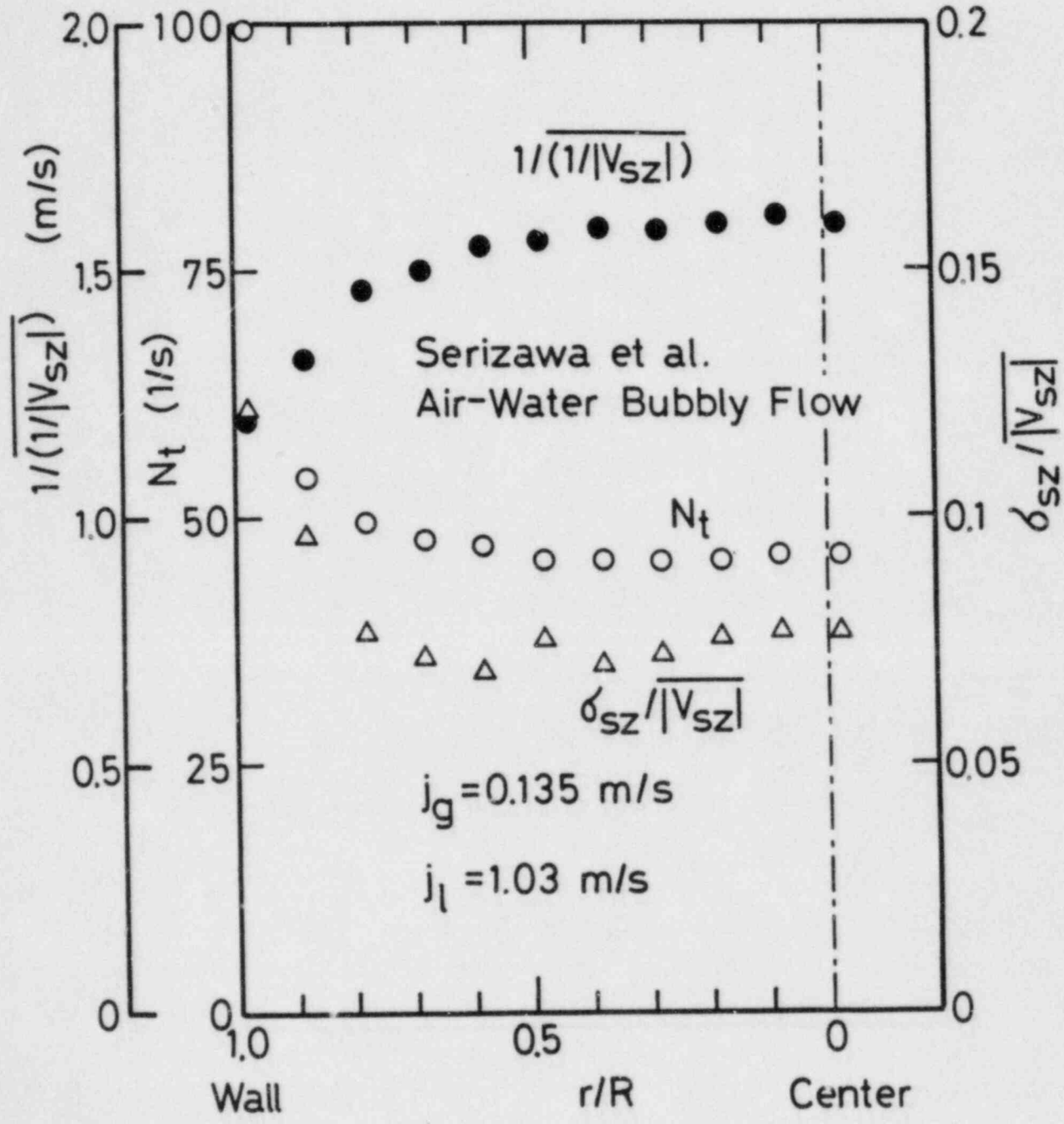

Fig. 9. Radial Profiles of N_t, $1/\overline{(1/|v_{sz}|)}$ and $\sigma_{sz}/\overline{|v_{sz}|}$ for Air-Water Bubbly Flow at j_g = 0.135 m/s and j_ℓ = 1.03 m/s (Serizawa et al. [55,57]

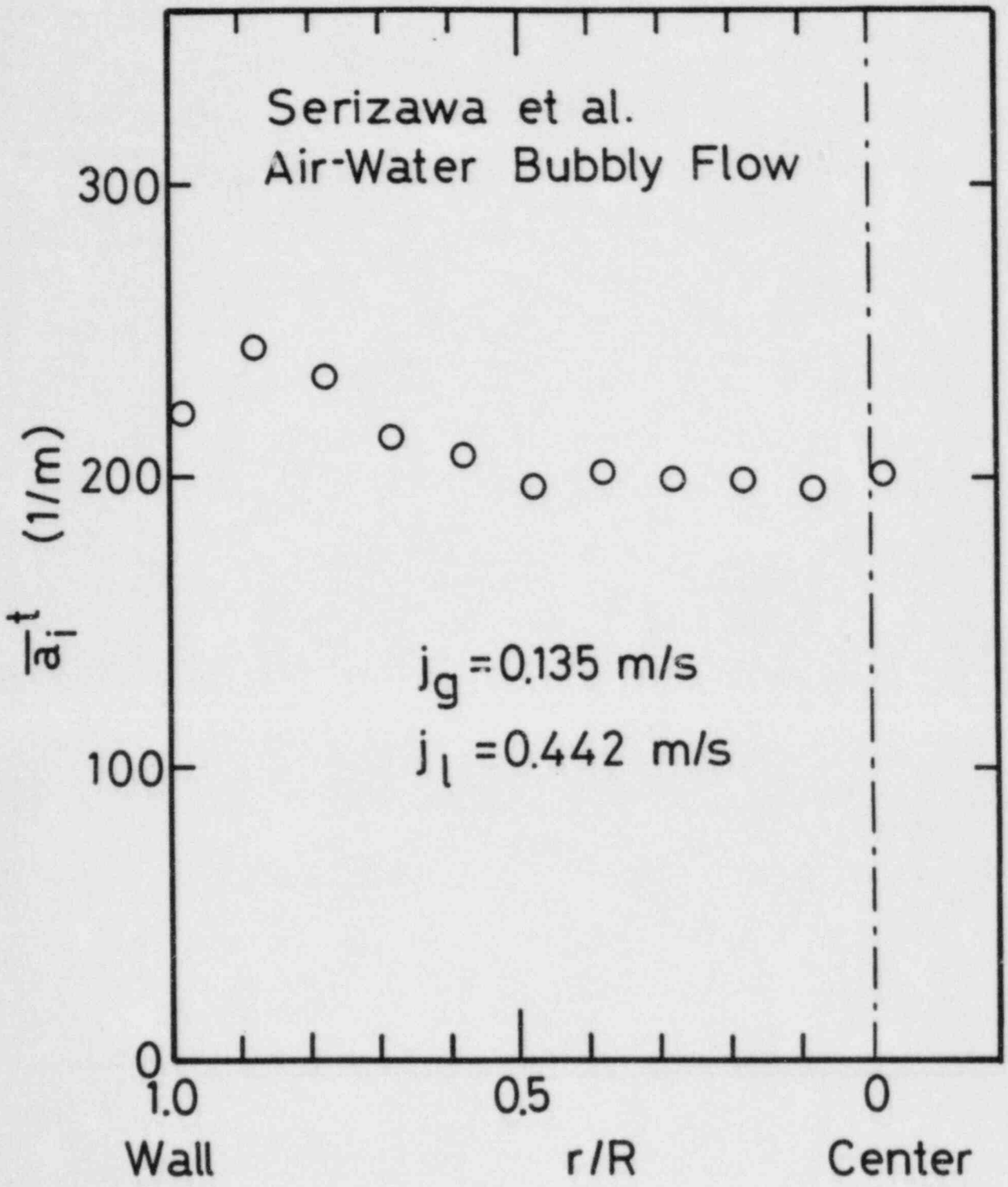

Fig. 10. Radial Profile of $\bar{a}_i^t$ for Air-Water Bubbly Flow at j_g = 0.135 m/s and j_ℓ = 0.442 m/s Calculated from the Data of Serizawa et al. [55, 57]

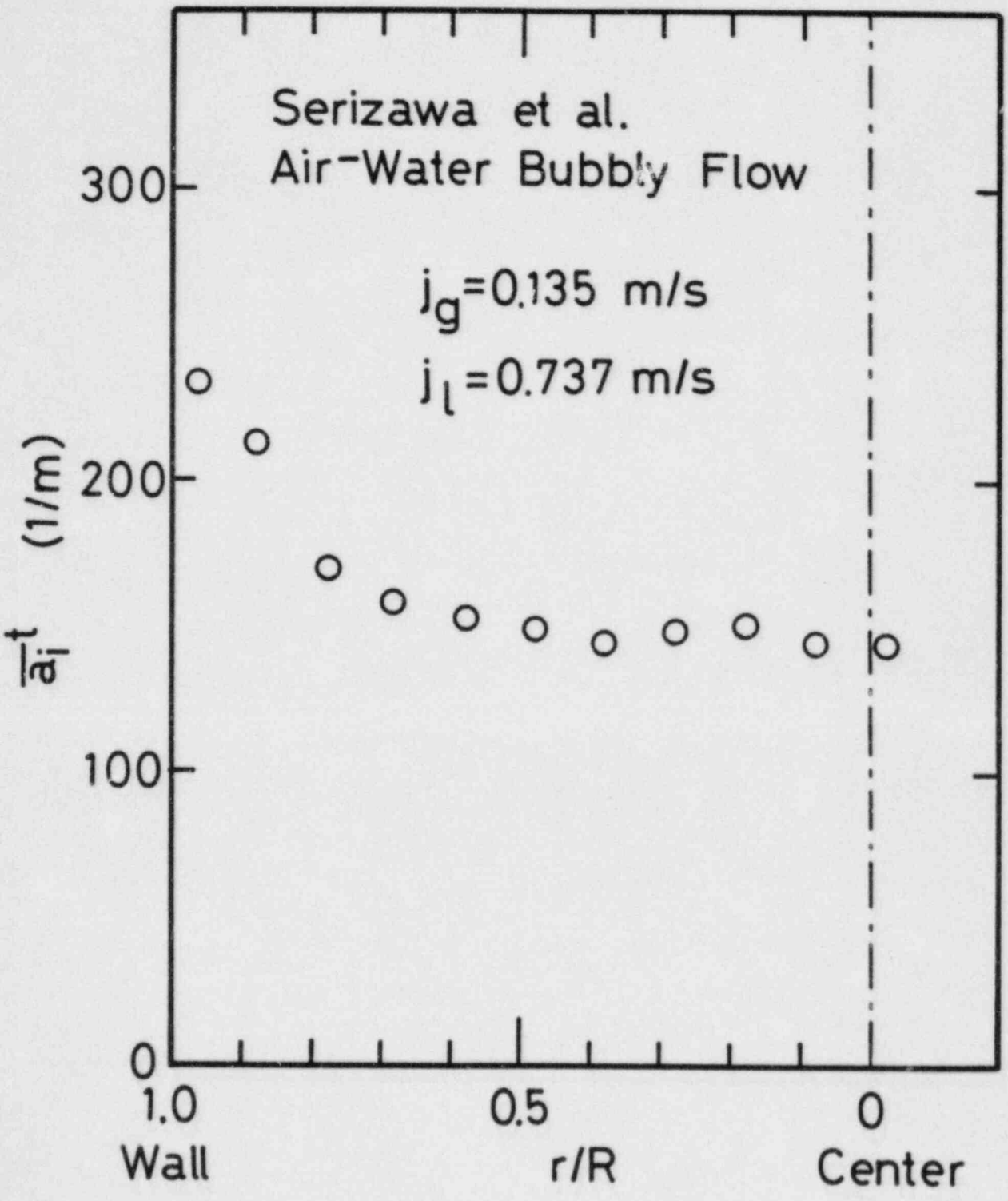

Fig. 11. Radial Profile of $\bar{a}_i^t$ for Air-Water Bubbly Flow at j_g = 0.135 m/s and j_ℓ = 0.737 m/s Calculated from the Data of Serizawa et al. [55, 57]

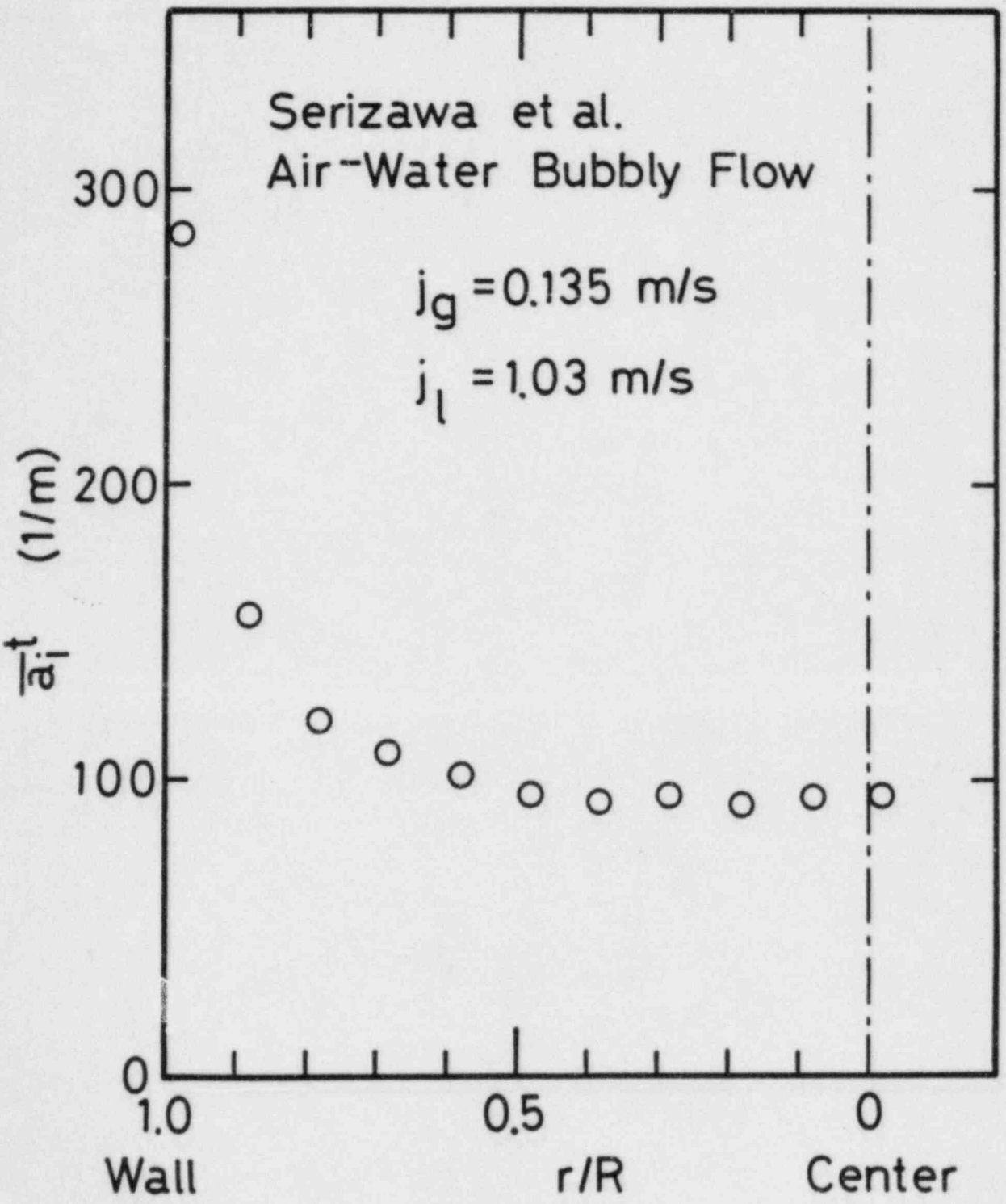

Fig. 12. Radial Profile of $\bar{a}_i^t$ for Air-Water Bubbly Flow at j_g = 0.135 m/s and j_ℓ = 1.03 m/s Calculated from the Data of Serizawa et al. [55, 57]

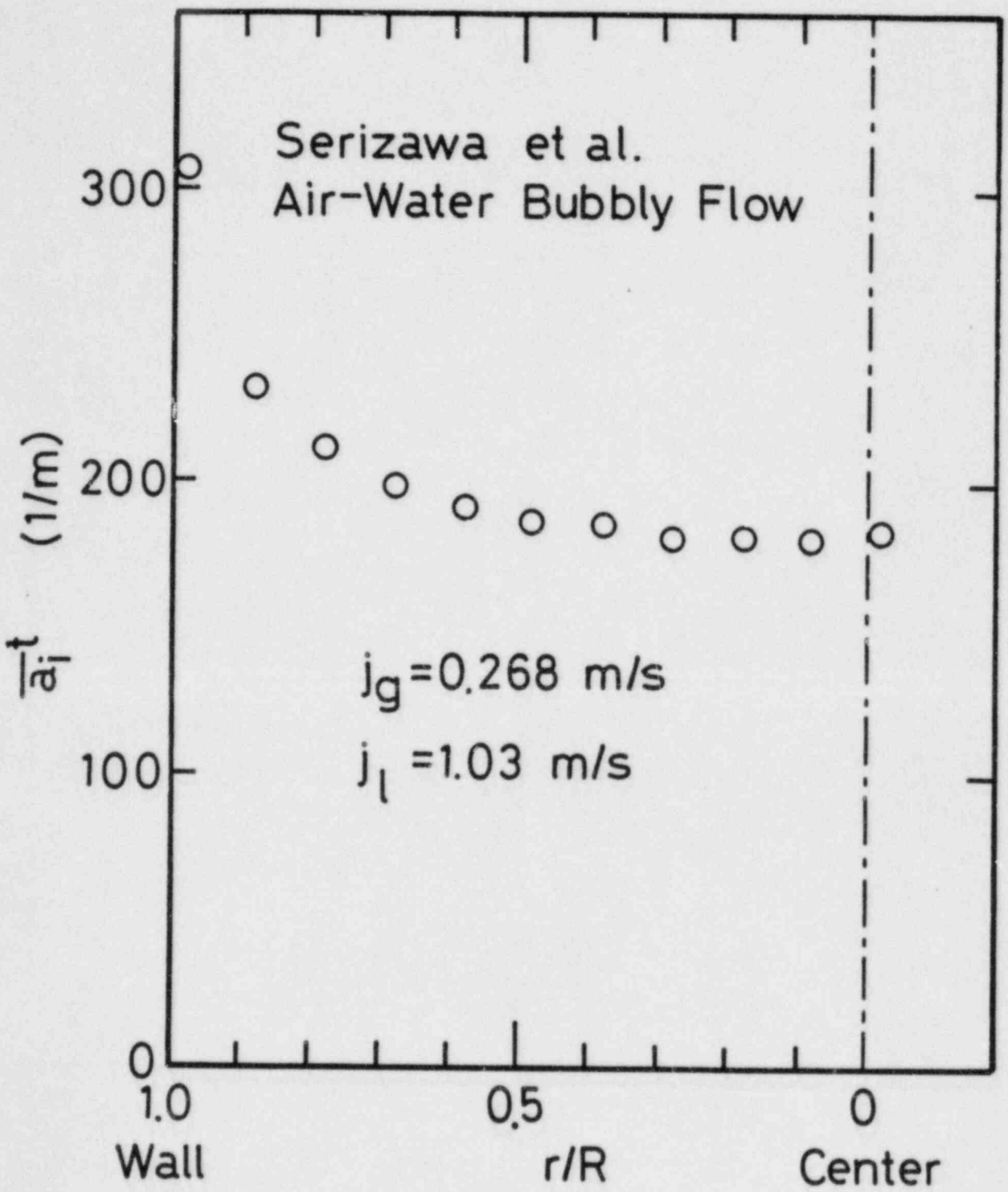

Fig. 13. Radial Profile of $\bar{a}_i^t$ for Air-Water Bubbly Flow at j_g = 0.268 m/s and j_ℓ = 1.03 m/s Calculated from the Data of Serizawa et al. [55, 57]

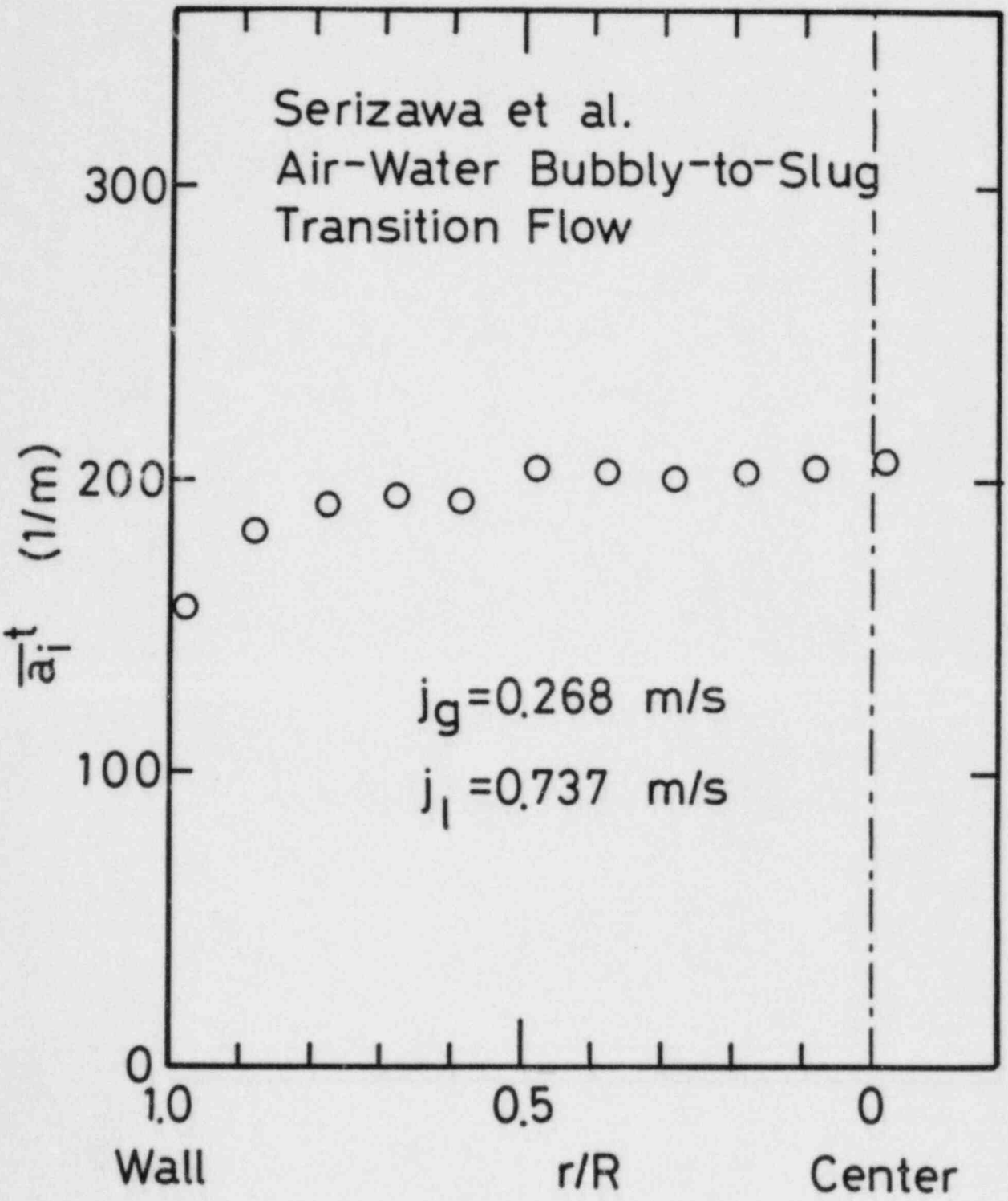

Fig. 14. Radial Profile of $\bar{a}_i^t$ for Air-Water Bubble-to-Slug-Transition Flow at j_g = 0.268 m/s and j_ℓ = 0.737 m/s Calculated from the Data of Serizawa et al. [55,57]

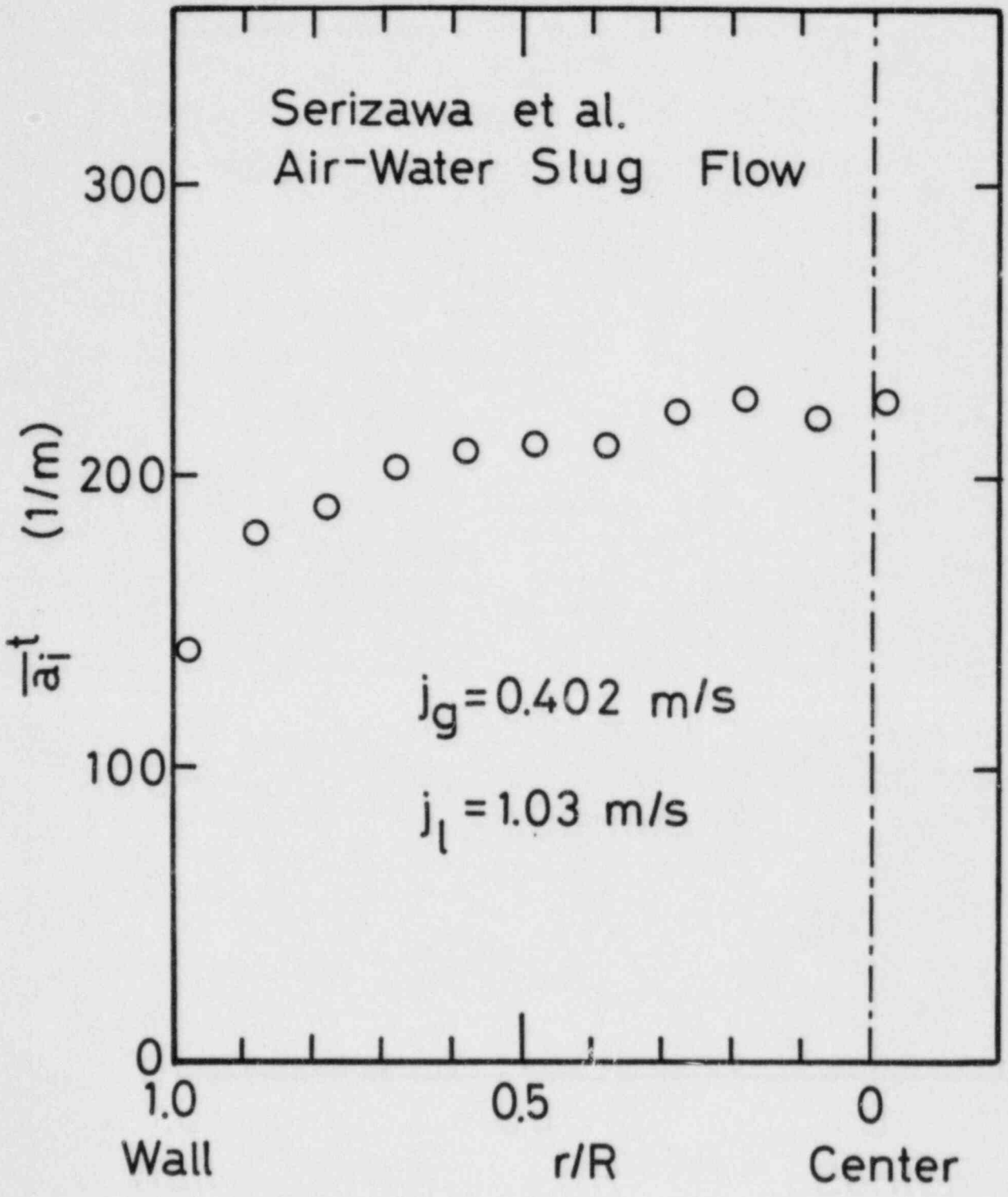

Fig. 15. Radial Profile of $\bar{a}_i^t$ for Air-Water Slug Flow at j_g = 0.402 m/s and j_ℓ = 1.03 m/s Calculated from the Data of Serizawa et al. [55,57]

the interfacial area concentration appear at the central region of the tube. It has been already shown by Ishii et al. [7] and Sekoguchi [53] that the area averaged interfacial area concentration is strongly dependent on two-phase flow regimes. However, the present study has demonstrated that a transverse profile of the local interfacial area concentration is also strongly dependent on the flow regimes. These results indicate that the interfacial transports of mass, momentum, and energy strongly depend on the overall flow regimes as well as on detailed transverse structures of flow.

Figure 16 shows the radial profiles of various local parameters of two-phase flow along with the interfacial area concentration. This figure suggests that the turbulent velocity of the liquid phase $\tilde{u}_\ell$ and the void fraction $\bar{\alpha}$ are closely related to the local interfacial area concentration as pointed out by Serizawa [59] and Herringe et al. [54].

Here the local interfacial area concentration has been calculated from Eqs. (103) and (117) using the experimental data obtained from one double-sensored probe. This procedure is based on several assumptions on statistical characteristics of the interface motion as described in the previous section, such as the randomness of the interfacial velocity and equilateral fluctuations of the velocity etc. These assumptions are considered to be valid in the central region of bubbly flow. However, in the very near wall region of bubbly flow or slug flow, some of the assumptions are not completely valid. Furthermore, for two-phase flow where fluid particles cannot be well defined, such as churn-turbulent flow, the above method may not be appropriate. For these circumstances, more information on the interfacial velocity is necessary for an accurate measurement of the local interfacial area concentration. The three double-sensored probe method which is described in the previous section is suitable for this purpose. Such detailed measurements are strongly recommended for a better understanding of two-phase flow structures and interfacial transport phenomena.

V. CONCLUSIONS

The local instantaneous formulation of the interfacial area concentration has been introduced based on the concept of a distribution. Using a delta function and the interface equation, the local instantaneous interfacial area concentration has been defined. Then by integrating the local instantaneous

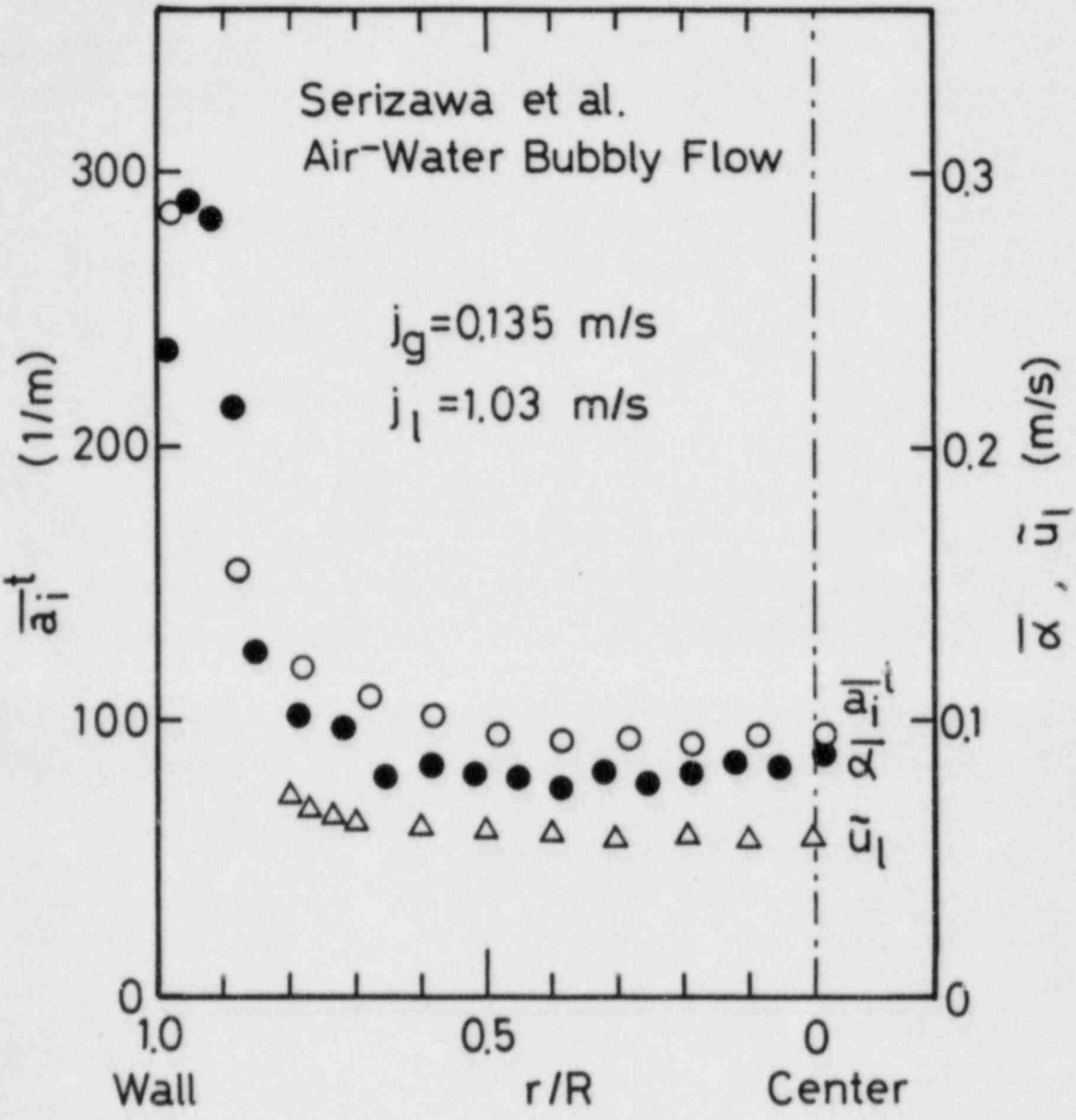

Fig. 16. Radial Profiles of $\bar{a}_i^t$, $\bar{\alpha}$ (Void Fraction) and $\tilde{u}_\ell$ (Turbulent Velocity of Liquid) at j_g = 0.135 m/s and j_ℓ = 1.03 m/s (Serizawa et al. [55,57])

interfacial area concentration, spatial and time averaged interfacial area concentrations have been obtained. For a dispersed two-phase flow the spatial (linear) averaged interfacial area concentration is given in terms of the number of interfaces per unit length and the harmonic mean of $\cos\theta_j$, where θ_j is the angle between the normal vector of jth interface and averaging direction. On the other hand, the time averaged interfacial area concentration is given in terms of the number of interfaces per unit time and the harmonic mean of $|\vec{v}_{ij}| \cos\phi_j$, where $|\vec{v}_{ij}|$ is the interfacial velocity of jth surface and ϕ_j is the angle between $\vec{v}_{ij}$ and the normal vector of jth interface.

Based on the local instantaneous formulation of the interfacial area concentration, several ergodic theorems concerning the averaged interfacial area concentration have been derived. The overall ergodic theorem for the time and spatial averages has been obtained theoretically. For a stationary and developed two-phase flow, the local ergodic theorem is obtained. Both theorems are important in terms of practical applications and interpretations of experimental data.

Based on these theoretical developments, several measurement methods for the interfacial area concentration have been proposed and discussed in detail. The method using three double-sensored probes located in three independent directions has been proposed for a general application. It is shown that this method enables an accurate measurement of the local interfacial area concentration. However, it is also pointed out that the required small size of the whole probe may be an engineering problem.

A much simpler method using one double-sensored probe is also proposed and discussed in detail. By assuming certain statistical characteristics of the interfacial motion, an expression for the local interfacial area concentration can be related to measurable quantities from a double-sensored probe.

Applying this one-probe method to experimental data, radial profiles of the local interfacial area concentration have been obtained for air-water bubbly and slug flow. The local interfacial area concentration has a peak value near the tube wall in the bubbly flow, while in slug flow it has higher values in the central region of two-phase flow. These results demonstrated the applicability of the one double-sensored probe method for the measurement of the local interfacial area concentration.

The formulation of the local interfacial area concentration and measuring methods developed in this study are basically applicable to any type of two-

phase flow. A further experimental study utilizing these methods for measuring the interfacial area concentration is highly desirable. Such a detailed measurement of the local quantities of two-phase flow greatly increases the understanding of interfacial transport phenomena, structures of two-phase flow and flow regimes.

ACKNOWLEDGMENTS

The authors would like to express their appreciation to Dr. N. Zuber and Mr. M. Young of NRC for valuable discussions on the subject.

A part of this work was performed under the auspices of the U.S. Nuclear Regulatory Commission.

REFERENCES

1. Zuber, N. and Findley, J. A., "Average Volumetric Concentration in Two-phase Flow Systems," J. Heat Trans. 87, 453 (1965).

2. Wallis, G. B., One-Dimensional Two-Phase Flow, McGraw-Hill Publishing Co., NY, 261-263 (1969).

3. Ishii, M., "One-Dimensional Drift-Flux Model and Constitutive Equations for Relative Motion between Phases in Various Flow Regimes," ANL-77-47 (1977).

4. Ishii, M., Thermo-fluid Dynamic Theory of Two-phase Flow, Eyrolles, Paris, Scientific and Medical Publication of France, NY (1975).

5. Delhaye, J. M., "Equations fondamentales des écoulements diphasiques, Parts 1 and 2," CEA-R-3429, France (1968).

6. Ishii, M. and Mishima, K., "Study of Two-Fluid Model and Interfacial Area," ANL-80-111, NUREG/CR-1873 (1980).

7. Ishii, M., Mishima, K., Kataoka, I., and Kocamustafaogullari, G., "Two-Fluid Model and Importance of the Interfacial Area in Two-Phase Flow Analysis," Proc. 9th U.S. National Congress of Applied Mechanics, 73-80, Ithaca, NY, June 21-25, 1982.

8. Sharma, M. M. and Mashelkar, R. A., "Absorption with Reaction in Bubble Columns," Inst. of Chem. Engrs., Symposium Series 28, Tripartite Chemical Engineering Conference, Montreal (1968).

9. Watson, A. P., Cormack, D. E., and Charles, M. E., "A Preliminary Study of Interfacial Areas in Vertical Cocurrent Two-phase Upflow," Can. J. Chem. Eng. 57, 16 (1979).

10. Shilimkan, R. V. and Stepanek, J. B., "Interfacial Area in Cocurrent Gas-Liquid Upward Flow in Tubes of Various Size," Chem. Eng. Sci. 32, 149 (1977).

11. Akita, K. and Yoshida, F., "Bubble Size, Interfacial Area, and Liquid-phase Mass Transfer Coefficient in Bubble Columns," Ind. Eng. Chem. Process Des. Dev. 13(1), 84 (1974).

12. Kasturi, G. and Stepanek, J. B., "Two-phase Flow-III. Interfacial Area in Cocurrent Gas-Liquid Flow," Chem. Eng. Sci. 29, 713-719 (1974).

13. Bier, K. et al., "Blasenbildung und Phasengrenzfläche beim Dispergieren von Gasen in Flussigkeiten an einzelnen Gaszulaufoffnungen, Teil 2: Einflutz von Systemdruck und Stoffeigenschaften auf die Blasengrobe und die spezifische Phasengrenzflache," Warme-und Stoffubertragung 11, 217 (1978).

14. Gregory, G. A. and Scott, D. S., "Physical and Chemical Mass Transfer in Horizontal Cocurrent Gas-Liquid Slug Flow," Proc. of Intl. Sym. on Res. in Cocurrent Gas-Liquid Flow, Waterloo (1968).

15. Shah, A. K. and Sharma, M. M., "Mass Transfer in Gas-Liquid (Horizontal) Pipeline Contactors," Can. J. Chem. Eng. 53, 572 (1975).

16. Wales, C. E., "Physical and Chemical Absorption in Two-phase Annular and Dispersed Horizontal Flow," AIChE J. 12(6), 1166 (1966).

17. Porter, K. E., King, M. B., and Varshney, K. C., "Interfacial Areas and Liquid-Film Mass-Transfer Coefficients for a 3 ft. Diameter Bubble Cap Plate Derived from Absorption Rates of Carbon Dioxide into Water and Cuastic Soda Solutions," Trans. Inst. Chem. Eng. 44, T274 (1966).

18. Dillion, G. B. and Harris, I. J., "The Determination of Mass Transfer Coefficients and Interfacial Areas in Gas-Liquid Contacting Systems," Can. J. Chem. Eng. 44, 307 (1966).

19. Abdel-Aal, H. K., Stiles, G. B., and Holland, C. D., "Formation of Interfacial Area at High Rates of Gas Flow through Submerged Orifices," AIChE J. 12(1), 174 (1966).

20. Burgess, J. M. and Calderbank, P. H., "The Measurement of Bubble Parameters in Two-phase Dispersions--II, The Structure of Sieve Tray Froths," Chem. Eng. Sci. 30, 1107 (1975).

21. Banerjee, S., Scott, D. S., and Rhodes, E., "Studies on Cocurrent Gas-Liquid Flow in Helically Coiled Tubes, II. Theory and Experiments on Turbulent Mass Transfer with and without Chemical Reaction," Can. J. Chem. Eng. 48, 542 (1970).

22. Kulic, E. and Rhodes, E., "Chemical Mass Transfer in Co-Current Gas-Liquid Slug Flow in Helical Coils," Can. J. Chem. Eng. 52, 114 (1974).

23. Robinson, C. W. and Wilke, C. R., "Simultaneous Measurement of Interfacial Area and Mass Transfer Coefficients for a Well-mixed Gas Dispersion in Aqueous Electrolyte Solutions," AIChE J. 20(2), 285 (1974).

24. Sridhar, T. and Potter, O. E., "Interfacial Area Measurements in Gas-Liquid Agitated Vessels--Comparison of Techniques," Chem. Eng. Sci. 33, 1347 (1978).

25. Sridharan, K. and Sharma, M. M., "New Systems and Methods for the Measurement of Effective Interfacial Area and Mass Transfer Coefficients in Gas-Liquid Contactors," Chem. Eng. Sci. 31, 767 (1976).

26. Mehta, V. D. and Sharma, M. M., "Mass Transfer in Mechanically Agitated Gas-Liquid Contactors," Chem. Eng. Sci. 26, 461 (1971).

27. Shende, B. W. and Sharma, M. M., "Mass Transfer in Packed Columns: Cocurrent Operation," Chem. Eng. Sci. 29, 1763 (1974).

28. Sharma, M. M. and Gupta, R. K., "Mass Transfer Characteristics of Plate Columns without Downcomer," Trans. Inst. Chem. Eng. 45, T169 (1967).

29. Mashelkar, R. A. and Sharma, M. M., "Mass Transfer in Bubble and Packed Bubble Columns," Trans. Inst. Chem. Eng. 48, T162 (1970).

30. Sharma, M. M. and Danckwerts, P. V., "Chemical Methods of Measuring Interfacial Area and Mass Transfer Coefficients in Two-fluid Systems," Br. Chem. Eng. 15(4), 522 (1970).

31. Trice, V. G., Jr. and Rodger, W. A., "Light Transmittance as a Measure of Interfacial Area in Liquid-Liquid Dispersions," AIChE J. 2(2), 205 (1956).

32. Landau, J. et al., "Comparison of Methods for Measuring Interfacial Areas in Gas-Liquid Dispersions," Can. J. Chem. Eng. 55, 13 (1977).

33. Calderbank, P. H., "Physical Rate Processes in Industrial Fermentation, Part I and Part II," Trans. Inst. Chem. Eng. 36, 443 (1958) and 37, 173 (1959).

34. Quigley, C. J., Johnson, A. I., and Harris, B. L., "Size and Mass Transfer Studies of Gas Bubbles," Chem. Eng. Progr. Sym. Series 51, 31 (1955).

35. Vermeulen, T., Williams, G. M., and Langlois, G. E., "Interfacial Area in Liquid-Liquid and Gas-Liquid Agitation," Chem. Eng. Progr. 51(2), 85-F (1955).

36. Tadaki, T. and Maeda, S., "On the CO_2 Desorption in the Gas Bubble Column," Trans. Japan chem. Eng. Soc. 27(11), 808 (1963).

37. Westerterp, K. R., van Dierendonck, L. L., and de Kraa, J. A., "Interfacial Areas in Agitated Gas-Liquid Contactors," Chem. Eng. Sci. 18, 157 (1963).

38. Yoshida, F. and Miura, Y., "Gas Absorption in Agitated Gas-Liquid Contactors," I&EC, Process and Des. Dev. 2(4), 263 (1963).

39. Ohba, K., "Measurement of Interfacial Area and Void Fraction in Bubbly Flow," 15th National Heat Transfer Sym. Japan, 331-333 (1978).

40. Veteau, J. M., "Contribution a L'etude des Techniques de Mesure de L'aire Interfaciale dans les Ecoulements a Bulles," Ph.D. Thesis, L'universite Scientifique et Medicale et L'institut National Polytechnique de Grenoble, (1981).

41. Banerjee, S. and Khachadour, A., "A Radioisotope Method for Interfacial Area Measurements in Two-Component Systems," J. Heat Trans. 103, 319 (1981).

42. Miller, D. N., "Interfacial Area, Bubble Coalescence and Mass Transfer in Bubble Column Reactors," AIChE J. 29(2), 312 (1983).

43. Kocamustafaogullari, G. and Ishii, M., "Interfacial Area and Nucleation Site Density in Boiling Systems," Int. J. Heat Mass Trans. 26(9), 312 (1983).

44. Schwartz, L., Methodes Mathematiques pour les Sciences Physiques, Editions Scientifiques Hermann, Paris (1961).

45. Schwartz, L., Théorie des Distributions I, II, Editions Scientifiques Hermann, Paris (1950-1951).

46. Dirac, P. A. M., The Principles of Quatum Mechanics, 4th Ed., Oxford Univ. Press (1958).

47. Delhaye, J. M., "Sur les Surfaces Volumiques Locale et Intégrale en Ecoulement Diaphasiques," C.R. Acad. Sc. Paris, t. 282, Série A, 243 (1976).

48. Delhaye, J. M., Giot, M., and Riethmuller, M. L., "Thermohydraulics of Two-Phase Systems for Industrial Design and Nuclear Engineering," Chapter 9, Hemisphere Pub. Co., NY (1980).

49. Hewitt, G. F. and Lovegrove, P. C., "Experimental Methods in Two-Phase Flow Studies," EPRI NP-118, Electrical Power Research Inst. (1976).

50. Banerjee, S. and Lahey, R. T., Jr., "Advances in Two-Phase Flow Instrumentation," Advances in Nucl. Sci. Tech., Vol. 13 ed. by Lewin, J. and Becker, M., 227-414, Plenum Press, NY (1981).

51. Sekoguchi, K., Fukui, H., Matsuoka, T., and Nishikawa, K., "Studies on Statistical Characteristics of Bubbles by Electrical Resistivity Probe (I)," Trans. JSME 40(336), 2295 (1974).

52. Sekoguchi, K., Fukui, H., Tutui, M., and Nishikawa, K., "Studies on Statistical Characteristics of Bubbles by Electrical Resistivity Probe (II)," Trans. JSME 40(336), 2302 (1974).

53. Sekoguchi, K., "Characteristics of Gas-Liquid Two-Phase Flow," Basic Principles and Applications of Multiphase Flow, ed. by Akagawa, K, 83, Japan Science Council (1982).

54. Herringe, R. A. and Davis, M. R., "Structural Development of Gas-Liquid Mixture Flows," J. Fluid Mech. 73, Part 1, 97 (1976).

55. Serizawa, A., "Fluid Dynamic Characteristics of Two-Phase Flow," Ph.D. Thesis, Kyoto Univ. (1974).

56. Serizawa, A., Kataoka, I., and Michiyoshi, I., "Turbulence Structure of Air-Water Bubbly Flow I. Measuring Techniques," Int. J. Multiphase Flow 2, 221 (1975).

57. Serizawa, A., Kataoka, I., and Michiyoshi, I., "Turbulence Structure of Air-Water Bubbly flow II. Local Properties," Int. J. Multiphae Flow, 2, 235 (1975).

58. Serizawa, A., Kataoka, I., and Michiyoshi, I., "Turbulence Structure of Air-Water Bubbly Flow III. Transport Properties," Int. J. Multiphase Flow 2, 247 (1975).

59. Serizawa, A., "Turbulence Structure of Bubbly Flow," Flow Characteristics and Applications of Multiphase Flow, ed. by Akagawa, K, 99, Japan Science Council (1983).

APPENDIX A

Product of Two Statistical Variables

By considering two statistical variables P_j and Q_j, a correlation coefficient of P_j and Q_j, which is denoted by γ_{PQ}, is defined as

$$\gamma_{PQ}^2 = \frac{\sum_{j=1}^{N} (P_j - \bar{P})(Q_j - \bar{Q})}{\left\{\sum_{j=1}^{N} (P_j - \bar{P})^2\right\}\left\{\sum_{j=1}^{N} (Q_j - \bar{Q})^2\right\}} \tag{A1}$$

where $\bar{P}$ and $\bar{Q}$ are means of P_j and Q_j. When P_j and Q_j are statistically independent, there are no correlation between P_j and Q_j. This implies

$$\gamma_{PQ} = 0 \tag{A2}$$

In this case, Eqs. (A1) and (A2) gives

$$\sum_{j=1}^{N} (P_j - \bar{P})(Q_j - \bar{Q}) = 0 \tag{A3}$$

On the other hand,

$$\sum_{j=1}^{N} (P_j - \bar{P})(Q_j - \bar{Q}) \equiv \sum_{j=1}^{N} P_j Q_j - N(\bar{P}\bar{Q}) \tag{A4}$$

because

$$\bar{P} = \frac{1}{N} \sum_{j=1}^{N} P_j \quad \text{and} \quad \bar{Q} = \frac{1}{N} \sum_{j=1}^{N} Q_j \tag{A5}$$

From Eqs. (A3) and (A4), one finally obtains

$$\overline{PQ} \equiv \frac{1}{N} \sum_{j=1}^{N} P_j Q_j$$

$$= \bar{P}\ \bar{Q} \qquad \text{(A6)}$$

Distribution for NUREG/CR-4029 (ANL-84-68)

Internal:

C. E. Till
R. Avery
J. F. Marchaterre
A. J. Goldman
P. A. Lottes
L. W. Deitrich
D. Rose
D. H. Cho
H. Komoriya
B. W. Spencer
W. A. Ragland
G. DeJarlais
D. P. Weber
W. T. Sha
Y. W. Shin
J. Sienicki
W. L. Chen
T. C. Chawla
T. Y. Wei
A. M. Tentner
M. Ishii (20)
ANL Patent Dept.
ANL Contract File
ANL Libraries (2)
TIS Files (6)

External:

NRC Washington, for distribution per R2 and R4 (335)
DOE-TIC (2)
Manager, Chicago Operations Office, DOE
Reactor Analysis and Safety Division Review Committee:

W. B. Behnke, Jr., Commonwealth Edison Co., P. O. Box 767, Chicago, Ill. 60690
W. P. Chernock, Combustion Engineering, Inc., 1000 Prospect Hill Road, Windsor, Conn. 06095
W. M. Jacobi, Westinghouse Electric Corp., P. O. Box 355, Pittsburgh, Pa. 15230
S. Levine, NUS Corp., 910 Clopper, Gaithersburg, Md. 20878
E. A. Mason, Standard Oil Co., P. O. Box 400, Naperville, Ill. 60566
W. F. Miller, Jr., Los Alamos National Lab., Los Alamos, N. M. 87545
M. J. Ohanian, University of Florida, Gainesville, Fla. 32611
J. J. Taylor, Electric Power Research Inst., P. O. Box 10412, Palo Alto, Calif. 94303

NRC FORM 335 (2 84) NRCM 1102 3201, 3202

U.S. NUCLEAR REGULATORY COMMISSION

BIBLIOGRAPHIC DATA SHEET

SEE INSTRUCTIONS ON THE REVERSE

1 REPORT NUMBER (Assigned by TIDC add Vol No., if any)

NUREG/CR-4029
ANL-84-68

2 TITLE AND SUBTITLE

Local Formulation of Interfacial Area Concentration and Its Measurements in Two-phase Flow

3 LEAVE BLANK

4 DATE REPORT COMPLETED

MONTH	YEAR
July	1984

5 AUTHOR(S)

I. Kataoka, M. Ishii, and A. Serizawa

6 DATE REPORT ISSUED

MONTH	YEAR
October	1984

7 PERFORMING ORGANIZATION NAME AND MAILING ADDRESS (Include Zip Code)

Argonne National Laboratory
9700 South Cass Avenue
Argonne, Illinois 60439

8 PROJECT/TASK/WORK UNIT NUMBER

8M406

9 FIN OR GRANT NUMBER

A2026

10 SPONSORING ORGANIZATION NAME AND MAILING ADDRESS (Include Zip Code)

Division of Accident Evaluation
Office of Nuclear Regulatory Research
U.S. Nuclear Regulatory Commission
Washington, D. C. 20555

11a TYPE OF REPORT

Technical

b PERIOD COVERED (Inclusive dates)

FY 1984

12 SUPPLEMENTARY NOTES

13 ABSTRACT (200 words or less)

The interfacial area concentration is one of the most important parameters in analyzing two-phase flow based on the two-fluid model. The local instantaneous formulation of the interfacial area concentration is introduced here. Based on this formulation, time and spatial averaged interfacial area concentrations are derived, and the local ergodic theorem (the equivalency of the time and spatial averaged values) is obtained for stationary developed two-phase flow. On the other hand, the global ergodic theorem is derived for general two-phase flow. Measurement methods are discussed in detail in relation to the present analysis. The three-probe method, with which local interfacial area concentration can be measured accurately, has been proposed. The one probe method under some statistical assumptions has also been proposed.

In collaboration with the experimental data for the interfacial velocity, radial profiles of the local interfacial area concentration are obtained based on the one probe method. The result indicates that the local interfacial area concentration has a peak value near the tube wall in bubbly flow, while in slug flow it shows a higher value in the central region of the tube for that particular set of data.

14 DOCUMENT ANALYSIS - a KEYWORDS/DESCRIPTORS

Interfacial Area
Two-phase Flow
Interfacial Transfer

b IDENTIFIERS/OPEN-ENDED TERMS

15 AVAILABILITY STATEMENT

Unlimited

16 SECURITY CLASSIFICATION

(This page) Unclassified

(This report) Unclassified

17 NUMBER OF PAGES

18 PRICE